CONDITION NUMBER ESTIMATES FOR COMBINED POTENTIAL INTEGRAL OPERATORS IN ACOUSTICS AND THEIR BOUNDARY ELEMENT DISCRETISATION

T BETCKE[*][†][**], S N CHANDLER-WILDE[*][‡][**], I G GRAHAM[§][**], S LANGDON[*][¶][**], AND M LINDNER[‖][**]

Abstract. We consider the classical coupled, combined-field integral equation formulations for time-harmonic acoustic scattering by a sound soft bounded obstacle. In recent work, we have proved lower and upper bounds on the L^2 condition numbers for these formulations, and also on the norms of the classical acoustic single- and double-layer potential operators. These bounds to some extent make explicit the dependence of condition numbers on the wave number k, the geometry of the scatterer, and the coupling parameter. For example, with the usual choice of coupling parameter they show that, while the condition number grows like $k^{1/3}$ as $k \to \infty$, when the scatterer is a circle or sphere, it can grow as fast as $k^{7/5}$ for a class of 'trapping' obstacles. In this paper we prove further bounds, sharpening and extending our previous results. In particular we show that there exist trapping obstacles for which the condition numbers grow as fast as $\exp(\gamma k)$, for some $\gamma > 0$, as $k \to \infty$ through some sequence. This result depends on exponential localisation bounds on Laplace eigenfunctions in an ellipse that we prove in the appendix. We also clarify the correct choice of coupling parameter in 2D for low k. In the second part of the paper we focus on the boundary element discretisation of these operators. We discuss the extent to which the bounds on the continuous operators are also satisfied by their discrete counterparts and, via numerical experiments, we provide supporting evidence for some of the theoretical results, both quantitative and asymptotic, indicating further which of the upper and lower bounds may be sharper.

1. Introduction. Consider scattering of a time-harmonic ($\mathrm{e}^{-\mathrm{i}\omega t}$ time dependence) acoustic wave u^i by a bounded, sound soft obstacle occupying a compact set $\Omega \subset \mathbb{R}^d$ ($d = 2$ or 3) with Lipschitz boundary Γ, which is such that the complement set $\Omega_e := \mathbb{R}^d \setminus \Omega$ is connected. The medium of propagation, occupying Ω_e, is assumed to be homogeneous, isotropic and at rest. Under the assumption that u^i is an entire solution of the Helmholtz (or reduced wave) equation with *wavenumber* $k = \omega/c > 0$ (where $c > 0$ denotes the speed of sound), we seek the resulting time-harmonic acoustic pressure field u, satisfying the Helmholtz equation

$$\Delta u + k^2 u = 0 \qquad \text{in} \qquad \Omega_e . \tag{1.1}$$

This is to be solved subject to the sound soft boundary condition

$$u = 0 \qquad \text{on} \qquad \Gamma = \partial \Omega_e, \tag{1.2}$$

and the Sommerfeld radiation condition, which requires that

$$\frac{\partial u^s}{\partial r} - \mathrm{i} k u^s = o(r^{-(d-1)/2}) \tag{1.3}$$

[*]Department of Mathematics and Statistics, University of Reading, Whiteknights, PO Box 220, Berkshire RG6 6AX, UK

[†]Email: `t.betcke@reading.ac.uk`

[‡]Email: `s.n.chandler-wilde@reading.ac.uk`

[§]Department of Mathematical Sciences, University of Bath, Bath BA2 7AY, UK. Email: `I.G.Graham@bath.ac.uk`

[¶]Email: `s.langdon@reading.ac.uk`

[‖]TU Chemnitz, Fakultät für Mathematik, 09107 Chemnitz, Germany. Email: `mali@hrz.tu-chemnitz.de`

as $r := |x| \to \infty$, uniformly in $\hat{x} := x/r$, where $u^s := u - u^i$ represents the scattered part of the field (see e.g. [12]). This problem has exactly one solution under the constraint that u and ∇u be locally square integrable; see e.g. [26].

In this paper we consider the two standard second kind boundary integral equation reformulations of (1.1)–(1.3). The first is the **indirect formulation**

$$A_{k,\eta}\varphi = g, \tag{1.4}$$

where

$$A_{k,\eta} := I + D_k - \mathrm{i}\eta S_k,$$

with $\eta \in \mathbb{R}\backslash\{0\}$ the *coupling parameter*, I the identity operator and S_k and D_k the *single-* and *double-layer potential operators*. These are defined for $\varphi \in L^2(\Gamma)$ by

$$S_k\varphi(x) := 2 \int_\Gamma \Phi(x, y) \, \varphi(y) \, ds(y), \quad x \in \Gamma, \tag{1.5}$$

and

$$D_k\varphi(x) := 2 \int_\Gamma \frac{\partial\Phi(x, y)}{\partial\nu(y)} \, \varphi(y) \, ds(y), \quad x \in \Gamma, \tag{1.6}$$

with $\partial/\partial\nu(y)$ the derivative in the normal direction, with the unit normal $\nu(y)$ directed into Ω_e, and $\Phi(x, y)$ the standard free-space fundamental solution of the Helmholtz equation. This is given by

$$\Phi(x, y) := \begin{cases} \frac{\mathrm{i}}{4}H_0^{(1)}(k|x - y|), & d = 2, \\[2ex] \dfrac{\mathrm{e}^{\mathrm{i}k|x-y|}}{4\pi|x - y|}, & d = 3, \end{cases} \tag{1.7}$$

for $x, y \in \mathbb{R}^d$, $x \ne y$, where $H_0^{(1)}$ is the Hankel function of the first kind of order zero. Finally, $g := -2u^i|_\Gamma = 2u^s|_\Gamma$.

The second formulation is the **direct formulation**

$$A'_{k,\eta}\frac{\partial u}{\partial\nu} = f, \tag{1.8}$$

where

$$A'_{k,\eta} := I + D'_k - \mathrm{i}\eta S_k,$$

with D'_k the integral operator defined, for $\varphi \in L^2(\Gamma)$, by

$$D'_k\varphi(x) := 2 \int_\Gamma \frac{\partial\Phi(x, y)}{\partial\nu(x)} \, \varphi(y) \, ds(y), \quad x \in \Gamma,$$

and

$$f(x) := 2\frac{\partial u^i}{\partial\nu}(x) - 2\mathrm{i}\eta u^i(x), \quad x \in \Gamma.$$

It is well known (see [9] for details, in particular regarding how classical results can be adapted to the general Lipschitz case) that, for $\eta \ne 0$, $A_{k,\eta}$ and $A'_{k,\eta}$ are invertible as operators on $L^2(\Gamma)$, and that

$$\|A'_{k,\eta}\| = \|A_{k,\eta}\|, \quad \|{A'_{k,\eta}}^{-1}\| = \|A_{k,\eta}^{-1}\|.$$

2

(Throughout the paper $\| \cdot \|$ denotes the L^2 norm on Γ.)

A question that has received much recent attention in the literature (see for example [3, 4, 5, 10, 11, 15, 17, 20, 21]) is that of determining how the conditioning of the two standard integral equation formulations, (1.4) and (1.8), depends on the wavenumber k, on the coupling parameter η, and on the shape of Γ. Specifically we are interested in upper and lower bounds on the (identical) condition numbers of $A_{k,\eta}$ and $A'_{k,\eta}$, given by

$$ \text{cond } A'_{k,\eta} = \text{cond } A_{k,\eta} = \|A_{k,\eta}\| \, \|A_{k,\eta}^{-1}\|, $$

and so we are interested in upper and lower bounds on the norms of $A_{k,\eta}$ and its inverse, and also on the norms $\|S_k\|$ and $\|D_k\|$.

In our recent paper [10], we derived estimates which, to some extent, make explicit the dependence of each of these norms on k, η and Γ, with an emphasis on understanding conditioning in the important but difficult and relatively neglected case where $k \to \infty$. For example, with the usual choice of coupling parameter $\eta = k$, while the condition numbers of $A_{k,\eta}$ and $A'_{k,\eta}$ grow like $k^{1/3}$ as $k \to \infty$ when the scatterer is a circle or sphere [15], we show in [10] that they grow like $k^{1/2}$ for a starlike polygon and as fast as $k^{7/5}$ for a class of 'trapping' obstacles. In this paper we prove further bounds sharpening and clarifying our previous results, in particular studying trapping obstacles in much more detail. A main focus of the present paper is also the boundary element discretisation of these operators. Our aims here are threefold: to provide supporting evidence for some of the theoretical results of [10] and of §2 via numerical experiments; to determine how sharp the quantitative upper and lower bounds on norms of [10] may be, particularly in the cases where there is a significant gap between the two; to determine the extent to which the bounds on the continuous operators are also satisfied by their discrete counterparts.

We begin in §2 by summarising the estimates at the continuous level derived in [10], together with previous related results in the literature. Also, in the 2D case, we sharpen the estimates from [10] at low frequencies, and prove that the choice of η in [21, 20] (based on analysis for a circular scatterer) guarantees a bounded condition number in the limit $k \to 0$ even for general Lipschitz Γ. But the main novelty of §2 is that we show that there exist trapping obstacles for which the condition numbers of $A_{k,\eta}$ and its adjoint grow as fast as $\exp(\gamma k)$, for some $\gamma > 0$, as $k \to \infty$ through some sequence. This result depends on exponential localisation bounds on so-called 'bouncing-ball' type [19] Laplace eigenfunctions in an ellipse. For completeness we provide a self-contained and relatively elementary proof of this exponential localisation in the appendix; for eigenfunction localisation results in much more general settings proved using related but much more technical arguments see [30].

In §3 we prove results about the relationship between the continuous integral operators and their discrete counterparts, i.e. matrices derived from standard Galerkin boundary element method (BEM) discretisations. In §4 we present numerical results showing Galerkin BEM approximations to $\|A_{k,\eta}\|$, $\|A_{k,\eta}^{-1}\|$, $\|S_k\|$ and $\|D_k\|$ for a variety of obstacles, each for a range of values of k and η. Finally in §5 we present some conclusions.

The results of the present paper and of [10] have direct relevance to the numerical performance of boundary integral methods, since the condition number of the discretization of (1.4) and (1.8) appears naturally as a measure of the difficulty of computing numerical solutions in practice. Moreover the results in [10], and more particularly our new results on trapping obstacles, have direct relevance to a recent

detailed $k-$explicit numerical analysis of hp boundary integral methods for general Helmholtz scattering problems in [24]. There it is shown (for example in [24, Corollary 3.18]) that, provided $\|A_{k,k}^{-1}\| \leq Ck^{\beta}$ with C and β independent of k, then an hp refinement strategy in which p grows logarithmically in k and h decreases like $k^{-1}\log k$ yields a Galerkin method which is free from "pollution" (i.e. the error is bounded by the best possible error in the finite element space, multiplied by a constant independent of k). Our analytical and numerical results are suggestive that $\|A_{k,k}^{-1}\| \leq Ck^{\beta}$ holds for some k-independent C and β not only for starlike obstacles, as considered previously in [11], but also for certain trapping obstacles. But also we prove in §2.5 that there exist Lipschitz obstacles for which the bound $\|A_{k,k}^{-1}\| \leq Ck^{\beta}$ does not hold for any C and β. We also note that the paper [27] (a companion paper to [24]) contains new decompositions of the combined potential operators $A_{k,\eta}$ and $A'_{k,\eta}$ which are crucial in the analysis of the hp methods in [24]. Of key importance there is the fact that the decomposition involves certain operators which map into spaces of functions which are analytic in a neighbourhood of Γ. However this analysis is rather different in flavour (and has different goals) from that of the present paper.

We flag that a related and complementary study of the same boundary integral equation formulations that we consider in this paper has been carried out recently in [6]. That paper includes, similarly to our §4, a numerical study relating to a range of geometries of 2D scatterers, but [6] has a different focus, namely an investigation, via computation of the numerical range of boundary element discretisations, of conditions which ensure that $A_{k,k}$ is coercive, and how its coercivity constant depends on k.

Finally we note that, in a similar vein to our §4, Warnick and Chew [34, 33, 32] study the conditioning of boundary element discretisations of the single-layer potential operator S_k via an approximate theoretical analysis and numerical experiments, obtaining simple explicit approximate upper and lower bounds for the condition number as a function of k and the discretisation step size for several canonical 2D geometries (a circle, crack and two parallel cracks) [32, Table 2].

2. Bounds on norms and condition numbers at the continuous level.

2.1. The case of a circle or sphere. Prior to [10], most research was focussed on the case when Γ is a circle or sphere, in which case Fourier analysis methods are possible.

For the case $d = 2$, when Γ is the unit circle, rigorous upper bounds on $\|A_{k,\eta}\|$ and $\|A_{k,\eta}^{-1}\|$ for the case $\eta = k$ (previously proposed as optimal for conditioning for the unit circle when $k \geq 1$ in e.g. [3, 4, 21]) were derived in [15] and are that, for all sufficiently large k,

$$\|A_{k,k}\| \leq Ck^{1/3}, \tag{2.1}$$

$$\|A_{k,k}^{-1}\| \leq 1, \tag{2.2}$$

with C a constant independent of k. (Combining (2.2) with Lemma 2.1 below we see that, in fact, $\|A_{k,k}^{-1}\| = 1$ for all sufficiently large k.) Although the focus in [15] was on bounding $A_{k,k}$ rather than on bounding the separate components S_k and D_k, Lemmas 4.1, 4.9 and 4.10 in [15] also imply the separate bounds that

$$\|S_k\| \leq Ck^{-2/3}, \quad \|D_k\| \leq Ck^{1/3}, \tag{2.3}$$

with C a constant independent of k.

For the case $d = 3$, when Γ is a sphere of unit radius, it is further shown in [15] that, for all sufficiently large k, (2.1) holds (see also [17]) and that, for every $C' > 1$,

$$\|A_{k,k}^{-1}\| \leq C',$$

for all sufficiently large k. A more refined and flexible upper bound on $A_{k,\eta}$ than (2.1) in the 3D case was recently derived in [5], where it was shown that, for all sufficiently large k,

$$\|D_k\| \leq C, \quad \|S_k\| \leq Ck^{-2/3}, \tag{2.4}$$

for some constant C independent of k, and hence

$$\|A_{k,\eta}\| = \|I + D_k - i\eta S_k\| \leq 1 + C\left(1 + |\eta|k^{-2/3}\right). \tag{2.5}$$

The choice $|\eta| = k$ yields the same estimate as (2.1), whereas the choice $|\eta| = k^{2/3}$ yields a k−independent bound for $\|A_{k,\eta}\|$.

2.2. The case of a starlike obstacle. Consider the case when Ω is connected, piecewise smooth and starlike, with Γ Lipschitz and C^2 in a neighbourhood of almost every $x \in \Gamma$, and

$$\delta_- := \operatorname*{ess\,inf}_{x \in \Gamma} \; x \cdot \nu(x) > 0$$

(assuming, without loss of generality, that the origin lies in Ω ($0 \in \Omega$)). Under these assumptions it is shown in [11] that, for $\eta \in \mathbb{R} \setminus \{0\}$,

$$\|A_{k,\eta}^{-1}\| \leq B, \tag{2.6}$$

where

$$B := \frac{1}{2} + \left[\left(\frac{\delta_+}{\delta_-} + \frac{4\delta^{*2}}{\delta_-^2}\right)\left[\frac{\delta_+}{\delta_-}\left(\frac{k^2}{\eta^2} + 1\right) + \frac{d-2}{\delta_-|\eta|} + \frac{\delta^{*2}}{\delta_-^2}\right] + \frac{(1 + 2kR_0)^2}{2\delta_-^2\eta^2}\right]^{1/2},$$

with

$$R_0 := \sup_{x \in \Gamma} |x|, \quad \delta_+ := \operatorname*{ess\,sup}_{x \in \Gamma} \; x \cdot \nu(x), \quad \delta^* := \operatorname*{ess\,sup}_{x \in \Gamma} |x - (x \cdot \nu(x))\nu(x)|.$$

These assumptions hold, for example, if Ω is a starlike polygon or polyhedron (and $0 \in \Omega$), and in these cases δ_- and δ_+ are the distances from the origin to the nearest and furthest sides of Γ, respectively. Note that the expression B blows up if $k/|\eta| \to \infty$ or if $\delta_+/\delta_- \to \infty$, or if $\delta_-|\eta| \to 0$, uniformly with respect to the values of other variables. If Γ is a circle or sphere, i.e. $\Gamma = \{x : |x| = R_0\}$, then $\delta_- = \delta_+ = R_0$ and $\delta^* = 0$ so

$$B = B_0 := \frac{1}{2} + \left[1 + \frac{k^2}{\eta^2} + \frac{d-2}{R_0|\eta|} + \frac{(1 + 2kR_0)^2}{2R_0^2\eta^2}\right]^{1/2}. \tag{2.7}$$

In the general case, since $\delta_- \leq \delta_+ \leq R_0$ and $0 \leq \delta_* \leq R_0$, it holds that $B \geq B_0$.

Based on low frequency asymptotics and numerical calculations for the case when Γ is a circle, it is proposed in [20] to choose

$$\eta = \max\left(\frac{1}{2R_0}, k\right) \tag{2.8}$$

to minimise the condition number of $A_{k,\eta}$ (and see [3, 4] for some further evidence supporting this choice). Based on computational experience, Bruno and Kunyansky [7, 8] recommend the similar formula that $\eta = \max(6T^{-1}, k/\pi)$, where T is the diameter of Ω, on the basis that this choice is found to minimise the number of GMRES iterations in an iterative solver. With either of these choices $\|A_{k,\eta}^{-1}\|$ is bounded uniformly in k for $k > 0$ for Ω starlike. In particular, with the choice (2.8) we see that

$$\|A_{k,\eta}^{-1}\| \le B \le \frac{1}{2} + \left[\left(\frac{\delta_+}{\delta_-} + \frac{4\delta^{*2}}{\delta_-^2}\right)\left[2\frac{\delta_+}{\delta_-} + \frac{2(d-2)R_0}{\delta_-} + \frac{\delta^{*2}}{\delta_-^2}\right] + \frac{8R_0^2}{\delta_-^2}\right]^{1/2}$$

$$\le \frac{1}{2} + \theta\left[4 + 13\theta + 4\theta^2\right]^{1/2}, \tag{2.9}$$

where $\theta = R_0/\delta_-$.

2.3. Upper bounds on $\|S_k\|$, $\|D_k\|$ and $\|A_{k,\eta}\|$ in the general Lipschitz case. It is shown in [10, Theorems 3.3, 3.5, 3.6], under the assumption that the scatterer Ω is Lipschitz, that there exist positive constants C_i, $i = 1, 2, 3$, dependent only on Ω, such that

$$\|S_k\| \le C_1 k^{(d-3)/2}, \tag{2.10}$$

$$\|D_k\| \le C_2 k^{(d-1)/2} + C_3, \tag{2.11}$$

$$\|A_{k,\eta}\| \le 1 + C_3 + C_2 k^{(d-1)/2} + C_1|\eta|k^{(d-3)/2}, \tag{2.12}$$

for $k > 0$. In 2D ($d = 2$), for the case Γ simply-connected and smooth, (2.12) was shown previously, for all sufficiently large k, in [15].

Expressions that are in principle computable for the constants C_i, $i = 1, 2, 3$, are given in [10]. In particular, in the simplest case that Γ is a straight line of length a, the upper bound on $\|S_k\|$ is given explicitly by

$$\|S_k\| \le 2\sqrt{\frac{a}{\pi k}}. \tag{2.13}$$

The bounds (2.10)–(2.12) are sharp in their dependence on k in the limit $k \to 0$ except for (2.10) (and so (2.12)) in the 2D case. In the 2D case the low frequency behaviour is more subtle, as studied previously for the case of a circle in [21, 20]. To obtain sharper bounds for low k for general Lipschitz Γ in the 2D case, note that, from the power series representations for Y_0 [1, (9.1.13)], it follows easily that

$$\left|Y_0(t) - \frac{2}{\pi}\log t\right| \le \frac{2}{\pi}\left\{\log 2 - \gamma + \frac{1}{4}\right\},$$

for $0 < t \le 1$, where $\gamma = 0.577\ldots$ is Euler's constant. Since also $|J_0(t)| \le 1$ for $t \ge 0$ [1, (9.1.18)], this implies that

$$\left|H_0^{(1)}(t) - \frac{2\mathrm{i}}{\pi}\log t\right| \le \sqrt{1 + \frac{4}{\pi^2}\left(\log 2 - \gamma + \frac{1}{4}\right)^2} < 1.03, \quad 0 < t \le 1. \tag{2.14}$$

(Since $H_0^{(1)}(t) = -\frac{2\mathrm{i}}{\pi}\log t + 1 + o(1)$ as $t \to 0^+$, this upper bound is an overestimate by not more than 3% for small t.)

Let S_0 denote the single-layer potential operator in the Laplace case, defined by (1.5) with $\Phi(x, y)$ replaced by $\Phi_0(x, y) := (1/2\pi)\log(R_0/|x-y|)$, for some constant

6

$R_0 > 0$ (later we will choose R_0 to be some characteristic length scale of Γ). It is a known result (e.g. [26]) that S_0 is a bounded operator on $L^2(\Gamma)$. Further, (2.14) implies that, where $D := \sup_{x,y \in \Gamma} |x - y|$ is the diameter of Γ,

$$\left| \Phi(x,y) - \Phi_0(x,y) + \frac{1}{2\pi} \log(kR_0) \right| < 0.26, \tag{2.15}$$

for $kD \leq 1$. From this inequality it follows that

$$\|S_k\| \leq \|S_0\| + \|S_k - S_0\| \leq \|S_0\| + \left(\frac{|\log kR_0|}{2\pi} + 0.26 \right) |\Gamma|,$$

for $kD \leq 1$, where $|\Gamma| = \int_\Gamma \mathrm{d}s$ is the length of Γ. Thus, taking $R_0 = 1$ in the above result, and combining this bound with (2.10), we obtain a refined version of (2.10) for small k when $d = 2$, that

$$\|S_k\| \leq C_0(1 - \log k), \quad \text{for } 0 < k \leq 1,$$

where the positive constant C_0 again depends only on Ω, which, combined with (2.11), gives that

$$\|A_{k,\eta}\| \leq 1 + C_3 + C_2 k^{1/2} + C_0|\eta|(1 - \log k), \quad 0 < k \leq 1. \tag{2.16}$$

2.4. Lower bounds on $\|S_k\|$, $\|D_k\|$ and $\|A_{k,\eta}\|$. The following lower bounds on $\|S_k\|$, $\|D_k\|$ and $\|A_{k,\eta}\|$ are derived in [10, §4].

LEMMA 2.1. *[10, Lemma 4.1] In both 2D and 3D, if a part of Γ is C^1, then $\|A_{k,\eta}\| \geq 1$, $\|A_{k,\eta}^{-1}\| \geq 1$.*

THEOREM 2.2. *[10, Theorem 4.2] In the 2D case, if Γ contains a straight line section of length a, then*

$$\|S_k\| \geq \sqrt{\frac{a}{\pi k}} + O(k^{-1})$$

as $k \to \infty$ and

$$\|A_{k,\eta}\| \geq |\eta| \sqrt{\frac{a}{\pi k}} - 1 + O(|\eta| k^{-1})$$

as $k \to \infty$, uniformly in η.

THEOREM 2.3. *[10, Theorem 4.4] In the 2D case, if Γ is locally C^2 in a neighbourhood of some point x^* on the boundary then, for some constants $C > 0$ and $k_0 > 0$, it holds for all $k \geq k_0$ and all $\eta \in \mathbb{R}$ that*

$$\|S_k\| \geq Ck^{-2/3} \quad and \quad \|A_{k,\eta}\| \geq C|\eta|k^{-2/3}.$$

More generally, adopt a local coordinate system OX_1X_2 with origin at x^* and the X_1 axis in the tangential direction at x^*, so that, near x^*, Γ coincides with the curve $\{x^* + t^*X_1 + n^*f(X_1) : X_1 \in \mathbb{R}\}$, for some $f \in C^2(\mathbb{R})$ with $f(0) = f'(0) = 0$; here t^* and n^* are the unit tangent and normal vectors at x^*. Then if, for some $N \in \mathbb{N}$, Γ is locally C^{N+1} near x^*, i.e. $f \in C^{N+1}(\mathbb{R})$, and if also $f'(0) = f^{(2)}(0) = \cdots = f^{(N)}(0) = 0$, then there exist $C > 0$ and $k_0 > 0$ such that

$$\|S_k\| \geq Ck^{-(N+1)/(2N+1)} \quad and \quad \|A_{k,\eta}\| \geq C|\eta|k^{-(N+1)/(2N+1)}$$

for all $k \geq k_0$ and all $\eta \in \mathbb{R}$.

In fact, under the conditions of Theorem 2.3, assuming further that $f^{(N+1)}(0) \neq 0$, we have quantitative lower bounds on $\|S_k\|$ and $\|A_{k,\eta}\|$:

$$\|S_k\| \geq C_N(0)\, k^{-(N+1)/(2N+1)}\, (1 + o(1)), \quad \text{as } k \to \infty,$$

and

$$\|A_{k,\eta}\| \geq \begin{cases} |\eta|\, C_N(0)\, k^{-(N+1)/(2N+1)}\, (1 + o(1)), & \text{if } |\eta| k^{-(N+1)/(2N+1)} \to \infty, \\ |\eta|\, C_N(0)\, k^{-(N+1)/(2N+1)} - \frac{N}{2\sqrt{2}} + o(1), & \text{if } |\eta| \approx k^{(N+1)/(2N+1)}, \end{cases}$$

as $k \to \infty$, where

$$C_N(0) = \sqrt{\frac{1}{8\pi}} \left(\sqrt{\frac{\pi}{2}} \frac{N!}{|f^{(N+1)}(0)|} \right)^{1/(2N+1)}.$$

Noting that $f''(0)$ is the curvature at x^*, we have the following corollary by applying these equations with $N = 1$.

COROLLARY 2.4. *[10, Corollary 4.5] Suppose (in the 2D case) that Γ is locally C^2 in a neighbourhood of some point x^* on the boundary and let R be the radius of curvature at x^*. If $R < \infty$, then,*

$$\|S_k\| \geq \frac{1}{2} \left(\frac{R}{\pi} \right)^{1/3} (2k)^{-2/3}(1 + o(1)), \quad \text{as } k \to \infty, \tag{2.17}$$

and

$$\|A_{k,\eta}\| \geq \begin{cases} \frac{|\eta|}{2} \left(\frac{R}{\pi} \right)^{1/3} (2k)^{-2/3}(1 + o(1)), & \text{if } |\eta| k^{-2/3} \to \infty, \\ \frac{|\eta|}{2} \left(\frac{R}{\pi} \right)^{1/3} (2k)^{-2/3} - \frac{1}{2\sqrt{2}} + o(1), & \text{if } |\eta| \approx k^{2/3}, \end{cases}$$

as $k \to \infty$.

We also have the following lower bounds on $\|D_k\|$. The conditions of Theorem 2.5 are satisfied, for example, if Γ is a polygon. (Choose x^1 to be a corner of the polygon and x^2 to be some point on an adjacent side, with Γ^1 a neighbourhood of x^1 on the adjacent side to x^2 and Γ^2.)

THEOREM 2.5. *[10, Theorem 4.6] In the 2D case, suppose x^1 and x^2 are distinct points on Γ, that Γ is C^1 in one-sided neighbourhoods Γ^1 and Γ^2 of x^1 and x^2, and that $(x^1 - x^2) \cdot \nu(x) = 0$ for $x \in \Gamma^2$ while $(x^1 - x^2)$ is not parallel to Γ^1 at x^1. Then, for some constants $C > 0$ and $k_0 > 0$, it holds for all $k \geq k_0$ that $\|D_k\| \geq Ck^{1/4}$.*

The conditions of the next theorem are satisfied with $N = 0$ by some pair of points x^1 and x^2 whenever Γ is C^1.

THEOREM 2.6. *[10, Theorem 4.7] In the 2D case, suppose x^1 and x^2 are distinct points on Γ, and that, for some $N \in \mathbb{N}_0 := \mathbb{N} \cup \{0\}$, Γ is C^1 and C^{N+1} in one-sided neighbourhoods Γ^1 and Γ^2 of x^1 and x^2, respectively, and that $x^1 - x^2$ is not parallel to Γ^1 at x^1. Without loss of generality, choose Γ^2 so that, for some $\tilde{\epsilon} > 0$ and $f \in C^{N+1}(\mathbb{R})$ with $f(0) = 0$,*

$$\Gamma^2 = \{x^2 + t\hat{u} + f(t)\hat{n} \,:\, 0 \leq t \leq \tilde{\epsilon}\}$$

where $\hat{u} = (x^2 - x^1)/|x^1 - x^2|$ and $\hat{n}$ are orthogonal unit vectors, and suppose that, for some $N \in \mathbb{N}_0$,

$$f^{(0)}(0) = f^{(1)}(0) = \cdots = f^{(N)}(0) = 0.$$

Then there exist $C > 0$ and $k_0 > 0$ such that

$$\|D_k\| \geq Ck^{N/(4N+4)}$$

for all $k > k_0$.

2.5. Lower bounds on $\|A_{k,\eta}^{-1}\|$ for trapping obstacles. In [10] it is shown that if Ω is a certain type of trapping obstacle then $\|A_{k,\eta}^{-1}\|$ can be unbounded as $k \to \infty$. The type of trapping obstacle considered in [10] is an obstacle for which there exists points P and Q on the boundary Γ such that:

(i) Γ is C^1 in neighbourhoods of P and Q;
(ii) the line segment joining P and Q lies in Ω_e and;
(iii) this line segment is normal to Γ at P and Q.

The line segment PQ is an example of a *periodic orbit*, by which we mean that it is the possible locus of a point billiard particle moving in the exterior region Ω_e in a straight line at unit speed as on an ideal billiard table, interacting with the boundary Γ according to the usual law of specular reflection (angle of reflection equals angle of incidence).

The specific class of trapping obstacle discussed in [10] is one for which Γ is a straight line locally to both P and Q. Precisely, the following theorem is proved, showing that $\|A_{k,\eta}^{-1}\|$ is unbounded as $k \to \infty$ for some class of trapping obstacles, at least provided $|\eta| \leq Ck$ for some constant C, which is the case of course for the standard choice $\eta = k$.

THEOREM 2.7. *[10, Theorem 5.1] There exists $C > 0$ such that, if Ω_e contains a square of side length $2a$, two parallel sides of which form part of Γ, and $\eta \in \mathbb{R} \setminus \{0\}$, then*

$$\|A_{k_m,\eta}^{-1}\| \geq C \, k_m^{9/10}\left(1 + \frac{|\eta|}{k_m}\right)^{-1}, \quad m \in \mathbb{N},$$

where $k_m := m\pi/2a$.

Theorem 2.7 relates to the case when the periodic orbit is between straight line parts of Γ. A key idea in its proof is the construction of a *quasimode* for the Helmholtz equation in Ω_e, by which we mean a function $v \in H^2(\Omega_e)$ which satisfies $\Delta v + k^2 v = g$ with $g \in L^2(\Omega_e)$ having a small norm relative to that of Δv; precisely, the quasimode is constructed, dependent on k, in such a way that if $k = k_m = m\pi/(2a)$ then $\|g\|_{L^2(\Omega_e)}/\|\Delta v\|_{L^2(\Omega_e)} = O(k^{-2})$ as $k \to \infty$. We note that the rate of growth of $\|A_{k,\eta}^{-1}\|$ predicted in Theorem 2.7 will be confirmed by numerical calculations in §4, and cf. [24, Fig. 4.7].

A periodic orbit between two parallel straight lines is neutrally stable, by which we mean that a small initial perturbation in the point billiard's position or direction will cause a perturbation to the billiard motion which grows at most linearly with time. If the parts of Γ neighbouring P and Q are curved slightly, so that the periodic orbit becomes stable, then the construction of a quasimode becomes possible for which $\|g\|_{L^2(\Omega_e)}/\|\Delta v\|_{L^2(\Omega_e)}$ decreases very rapidly as $k \to \infty$ through some unbounded sequence of values (see [19, 23] and the references therein), which leads to a very fast growth in $\|A_{k,\eta}^{-1}\|$ as $k \to \infty$ through the same sequence of values.

We will prove this statement in Theorem 2.8 below in a case for which a complete proof can be given by fairly elementary arguments. This simplest case is that in which the parts of Γ neighbouring P and Q form part of the boundary of an ellipse, precisely an ellipse of which PQ is the shortest periodic orbit, in which case the

quasimode can be constructed by perturbing a so-called *bouncing ball mode* (see [19]) eigenfunction of the ellipse. This mode can be written down explicitly in terms of Mathieu functions and can be shown to be exponentially localised around the stable periodic orbit PQ. (For details see the appendix, and for a visualization of several of these eigenfunctions see Figure 4.3 below.) An example of an exterior domain Ω_e and the corresponding scattering object Ω which satisfies the conditions of Theorem 2.8 is the obstacle labeled 'Elliptic cavity' in Figure 4.1 below.

THEOREM 2.8. *If, for some $a_1 > a_2 > 0$, Ω_e contains the ellipse $E := \{(x_1, x_2) : (x_1/a_1)^2 + (x_2/a_2)^2 < 1\}$, and if Γ coincides with the boundary of this ellipse in neighbourhoods of the points $(0, \pm a_2)$, then there exists a sequence $0 < k_0 < k_1 < k_2 < \ldots$, with $k_m \to \infty$ as $m \to \infty$, such that, for some $\gamma > 0$ and $C > 0$,*

$$\|A_{k_m,\eta}^{-1}\| \geq C\mathrm{e}^{\gamma k_m} \left(1 + \frac{|\eta|}{k_m}\right)^{-1}, \tag{2.18}$$

for $\eta \in \mathbb{R} \setminus \{0\}$ and $m = 0, 1, 2, \ldots$.

Proof. In the appendix we focus on a particular subset of the eigenfunctions of the Laplace operator with Dirichlet boundary conditions in the ellipse E. These are the functions $u_{m,0} \in C^2(\bar{E})$, $m = 0, 1, \ldots$, defined by $u_{m,0}(x) = \mathrm{Mc}_0^{(1)}(\mu, q_m)\mathrm{ce}_0(\nu, q_m)$, $x \in E$, where the elliptic coordinates (μ, ν) and standard Mathieu function notation are as defined in the appendix. The important property of the function $u_{m,0}$ is that it satisfies the eigenproblem (A.1) for wavenumber $k = k_m$, where $k_m = 2\sqrt{q_m/(a_1^2 - a_2^2)}$ and q_m is the $(m+1)$th positive solution of the equation (A.6) in the case $n = 0$, with $q_m \to \infty$ (so that $k_m \to \infty$) as $m \to \infty$. It is shown in the appendix (see (A.16)) that this particular subset of eigenfunctions $u_{m,0}$, $m = 0, 1, \ldots$, is a family of bouncing ball modes, with $u_{m,0}$ becoming increasingly localized around the periodic orbit $O := \{(0, x_2) : |x_2| \leq a_2\}$ as $m \to \infty$.

We will now construct a quasimode v_m on Ω_e by a suitable modification and extension of $u_{m,0}$. Let $\chi \in C^\infty(\mathbb{R}^2)$ be compactly supported and such that $\chi(x) = 1$ in some neighbourhood of O while $\chi(x) = 0$ in some neighbourhood of $\partial E \backslash \Gamma$. Abbreviate $u_{m,0}$ as u_m and define $v_m \in C^2(\bar{\Omega}_e)$ by $v_m(x) := \chi(x)u_m(x)$, $x \in \bar{E}$, $v_m(x) := 0$, $x \in \Omega_e \setminus E$. Then, in Ω_e,

$$\Delta v_m + k_m^2 v_m = g_m,$$

where $g_m(x) = 0$ for $x \in \Omega_e \setminus E$, while

$$g_m = u_m \Delta\chi + 2\nabla\chi \cdot \nabla u_m$$

in E. Let $E_- := \{x \in E : |x_1| > \epsilon_-\}$ and $E_+ := \{x \in E : |x_1| > \epsilon_+\}$, where $\epsilon_- > \epsilon_+ > 0$ are chosen sufficiently small so that $\chi = 1$ in $E \setminus E_-$. Then, where $\|.\|_\infty$ denotes the usual supremum norm on $C(\bar{E})$ and $\|\cdot\|_2$ the usual norm on $L^2(E)$ and $\|\cdot\|_{L^2(E_\pm)}$ the L^2 norm on $E_\pm$, we see that

$$\|g_m\|_2 \leq \|u_m\|_{L^2(E_-)}\|\chi\|_\infty + 2\|\nabla\chi\|_\infty\|\nabla u_m\|_{L^2(E_-)}.$$

In the remainder of the proof let C denote a positive constant, whose value does not depend on m, but which is not necessarily the same at each occurrence. By (A.16), for some $\beta > 0$,

$$\|u_m\|_{L^2(E_\pm)} \leq C\mathrm{e}^{-\beta k_m}\|u_m\|_2, \tag{2.19}$$

10

for $m = 0, 1, \ldots$. Further, $\|\nabla u_m\|_{L^2(E_-)}$ can be bounded by a constant multiple of $k_m \|u_m\|_{L^2(E_+)}$, so that

$$\|g_m\|_2 \leq C k_m \mathrm{e}^{-\beta k_m} \|u_m\|_2, \quad m = 0, 1, \ldots. \tag{2.20}$$

To see this last claim choose $f \in C^1(\mathbb{R})$ such that: (i) $1 \geq f(s) \geq 0$ for $s \in \mathbb{R}$; (ii) $f(s) = 0$ for $|s| \leq \epsilon_+$; (iii) $f(s) = 1$ for $|s| \geq \epsilon_-$; (iv) for some constant $M > 0$, $|f'(s)|/(f(s))^{1/2} \leq M$ for all $s \in \mathbb{R}$ for which $f(s) > 0$. (This can be achieved by defining f by $f(s) = P((|s|-\epsilon_+)/(\epsilon_- -\epsilon_+))$ for $\epsilon_+ \leq |s| \leq \epsilon_-$, where $P(t) = t^2(3-2t)$.) Define $\tilde{\chi} \in C^1(\bar{E})$ by $\tilde{\chi}(x) = f(x_1)$, $x \in \bar{E}$, and note that $1 \geq \tilde{\chi}(x) \geq 0$, for $x \in E$, that $\tilde{\chi}(x) = 0$ for $x \in E \setminus E_+$ and $\tilde{\chi}(x) = 1$ for $x \in E_-$, and that $|\nabla\tilde{\chi}(x)|/\sqrt{\tilde{\chi}(x)} \leq M$ for all $x \in E$ for which $\tilde{\chi}(x) > 0$. Now, by Green's theorem and since u_m is an eigenfunction in E,

$$k_m^2 \int_E \tilde{\chi} u_m^2 dx = -\int_E \tilde{\chi} u_m \Delta u_m \, dx = \int_E \nabla(\tilde{\chi} u_m) \cdot \nabla u_m \, dx,$$

so that

$$\int_E \tilde{\chi}(\nabla u_m)^2 dx \leq k_m^2 \int_{E_+} u_m^2 dx + M \int_E \sqrt{\tilde{\chi}} \, |\nabla u_m| \, u_m \, dx.$$

Applying Cauchy-Schwarz and noting that $2ab \leq \eta a^2 + \eta^{-1} b^2$, for all $\eta > 0$ and $a, b \geq 0$, we see that

$$\|\sqrt{\tilde{\chi}} \nabla u_m\|_2^2 \leq k_m^2 \|u_m\|_{L^2(E_+)}^2 + \frac{M\eta}{2} \|\sqrt{\tilde{\chi}} \nabla u_m\|_2^2 + \frac{M}{2\eta} \|u_m\|_{L^2(E_+)}^2,$$

for all $\eta > 0$. Choosing $\eta = M^{-1}$ we see that

$$\|\nabla u_m\|_{L^2(E_-)} \leq \|\sqrt{\tilde{\chi}} \nabla u_m\|_2 \leq c_m \|u_m\|_{L^2(E_+)},$$

where $c_m := \sqrt{M^2 + 2k_m^2}$.

Next note that

$$\|v_m\|_2^2 \geq \int_{E \setminus E_+} u_m^2 \, dx = \|u_m\|_2^2 - \|u_m\|_{L^2(E_+)}^2 \geq \frac{1}{4} \|u_m\|_2^2, \tag{2.21}$$

for all sufficiently large m, by (2.19). Thus, and noting (2.20),

$$\|\Delta v_m\|_2 = \|k_m^2 v_m - g_m\|_2 \geq k_m^2 \|v_m\|_2 - \|g_m\|_2 \geq \frac{k_m^2}{4} \|u_m\|_2,$$

for all sufficiently large m. Combining this bound with (2.20) we see that

$$\frac{\|g_m\|_{L^2(\Omega_e)}}{\|\Delta v_m\|_{L^2(\Omega_e)}} = \frac{\|g_m\|_2}{\|\Delta v_m\|_2} \leq C k_m^{-1} \mathrm{e}^{-\beta k_m} \leq C \mathrm{e}^{-\gamma k_m}, \; m = 0, 1, \ldots, \tag{2.22}$$

for some $0 < \gamma < \beta$.

To see that (2.22) induces exponential growth of $\|A_{k_m, \eta}^{-1}\|$, we proceed as in the proof of [10, Theorem 5.1] and define $v_m^i \in C(\mathbb{R}^2) \cap H_{\mathrm{loc}}^2(\mathbb{R}^2)$ by

$$v_m^i(x) := \int_E \Phi_{k_m}(x, y) g_m(y) \, dy, \quad x \in \mathbb{R}^2, \tag{2.23}$$

11

where Φ_{k_m} denotes the fundamental solution Φ of the Helmholtz equation in 2D in the case $k = k_m$. Then we can view $v_m \in C^2(\bar{\Omega}_e)$ as the total field for the problem of scattering by the obstacle Ω in the case when v_m^i is the incident field. For defining $v_m^s := v_m - v_m^i$ it holds that $\Delta v_m^s + k_m^2 v_m^s = 0$ in Ω_e, that v_m^s satisfies the Sommerfeld radiation condition (since v_m^i does and v_m is compactly supported), and that $v_m^s = -v_m^i$ on Γ. It follows, arguing as in the proof of [10, Theorem 5.1], that

$$A'_{k_m,\eta} \frac{\partial v_m}{\partial \nu} = f_m$$

(cf. (1.8)), where

$$f_m(x) := 2\frac{\partial v_m^i}{\partial \nu}(x) - 2i\eta v_m^i(x), \quad x \in \Gamma. \tag{2.24}$$

Since $\|A_{k_m,\eta}^{-1}\| = \|(A'_{k_m,\eta})^{-1}\|$, our proof of (2.18) will be completed if we can show that, for some constant $\gamma > 0$,

$$\left\| \frac{\partial v_m}{\partial \nu} \right\|_{L^2(\Gamma)} \geq C e^{\gamma k_m} \left(1 + \frac{|\eta|}{k_m} \right)^{-1} \|f_m\|_{L^2(\Gamma)}, \tag{2.25}$$

for $m = 0, 1, \dots$ and $\eta \in \mathbb{R} \setminus \{0\}$.

To see that (2.22) implies (2.25), we use (2.23), and we also apply Green's representation theorem [13] to v_m to give that

$$v_m(x) = \int_{\Omega_e} \Phi_{k_m}(x, y) g_m(y) \, dy + \int_{\Gamma} \Phi_{k_m}(x, y) \frac{\partial v_m}{\partial \nu}(y) \, ds(y), \quad x \in \Omega_e. \tag{2.26}$$

Using the bound (e.g. [10]) that $|H_0^{(1)}(t)| \leq \sqrt{2/(\pi t)}$, for $t > 0$, which implies that

$$|\Phi_{k_m}(x, y)| \leq (8\pi k_m |x - y|)^{-1/2},$$

we easily deduce from (2.26) that

$$\|v_m\|_2 \leq C k_m^{-1/2} \left(\|g_m\|_2 + \left\| \frac{\partial v_m}{\partial \nu} \right\|_{L^2(\Gamma)} \right),$$

for $m = 0, 1, \dots$. Combining this bound with (2.20) and (2.21) we see that

$$\left\| \frac{\partial v_m}{\partial \nu} \right\|_{L^2(\Gamma)} \geq C k_m^{1/2} \|u_m\|_2, \tag{2.27}$$

for $m = 0, 1, \dots$. Similarly, it follows from (2.23) that

$$\|v_m^i\|_{L^2(\Gamma)} \leq C k_m^{-1/2} \|g_m\|_2, \tag{2.28}$$

and that

$$\nabla v_m^i(x) = w_m^{(0)}(x) + w_m^{(1)}(x),$$

where, for $x \in \mathbb{R}^2$,

$$w_m^{(0)}(x) := \int_E \nabla_x \Phi_0(x, y) g_m(y) \, dy, \quad w_m^{(1)}(x) := \int_E \nabla_x \left(\Phi_{k_m}(x, y) - \Phi_0(x, y) \right) g_m(y) \, dy,$$

12

and (cf. §2.3) $\Phi_0(x,y) := (1/2\pi)\log(1/|x-y|)$ is the standard fundamental solution of the Laplace equation. Now, from standard mapping properties of Newtonian potentials, it holds that $w_m^{(0)} \in H^1(E)$, with $\|w_m^{(0)}\|_{H^1(E)} \le C\|g_m\|_2$. Hence, by the boundedness of the standard trace operator from $H^1(E)$ to $H^{1/2}(\partial E) \supset L^2(\partial E)$, it follows that $\|w_m^{(0)}\|_{L^2(\partial E)} \le C\|g_m\|_2$. Further it holds (see e.g. [10, equation (3.9)]) that

$$|\nabla_x(\Phi_0(x,y) - \Phi_{k_m}(x,y))| \le C\sqrt{\frac{k_m}{|x-y|}},$$

from which it follows (cf. (2.28)) that

$$\|w_m^{(1)}\|_{L^2(\partial E)} \le C k_m^{1/2}\|g_m\|_2.$$

Hence

$$\left\|\frac{\partial v_m^i}{\partial \nu}\right\|_{L^2(\Gamma)} \le C k_m^{1/2}\|g_m\|_2,$$

and combining this bound with (2.28) and the definition (2.24) of f_m, we see that

$$\|f_m\|_{L^2(\Gamma)} \le C k_m^{1/2}\left(1 + \frac{|\eta|}{k_m}\right)\|g_m\|_2.$$

Finally, combining this bound with (2.20) and (2.27), we see that

$$\|f_m\|_{L^2(\Gamma)} \le C k_m e^{-\beta k_m}\left(1 + \frac{|\eta|}{k_m}\right)\left\|\frac{\partial v_m}{\partial \nu}\right\|_{L^2(\Gamma)},$$

which implies that (2.25) holds for $\gamma < \beta$. $\square$

2.6. Choice of η for low k. Although the main focus of this paper is on conditioning in the limit as $k \to \infty$, for completeness we briefly address the limit $k \to 0$ in this section. Conditioning in this limit was explored carefully already in the papers [21, 20] where, for the case when Γ is a sphere or circle, precise asymptotic calculations were made of the choice of η which minimises cond $A_{k,\eta}$ in the limit $k \to 0$. The recommendations in these papers are for a circle/sphere of unit radius, and imply for a circle/sphere of radius $R_0 > 0$ that the optimal choices of η are

$$\eta = \begin{cases} \frac{1}{2R_0} + O(k^2 \log k), & d = 3, \\ \{\pi^2 + 4(\log(k/2) + \gamma)^2\}^{-1/2}\{1 + O(k^2 \log kR_0)\}, & d = 2, \end{cases} \tag{2.29}$$

where $\gamma = 0.577\ldots$ is Euler's constant. We will explain in this section why these choices, for any $R_0 > 0$, ensure a bounded condition number of $A_{k,\eta}$ as $k \to 0$ in the case of general Lipschitz Γ.

To understand this limit we need to recall what is known about integral equation formulations for the Laplace case $k = 0$. Let Φ_0 denote the fundamental solution of the Laplace equation, given simply by (1.7) with $k = 0$ in the 3D case, and defined as in §2.3 in the 2D case. Let S_0 and D_0 denote the single and double-layer potentials in the Laplace case, defined by equations (1.5) and (1.6) with S, D, and Φ replaced by S_0, D_0 and Φ_0. It is a fairly straightforward calculation (see e.g. [10] for the detail in the case of Lipschitz Γ) that

$$\|D_k - D_0\| \to 0 \text{ and } \|S_k - S_0\| \to 0 \tag{2.30}$$

as $k \to 0$ in the 3D case, and that the first of these results holds also in the 2D case. In the 2D case the limiting behaviour of S_k is more subtle. We see from (2.15) that

$$\left\| S_k - S_0 + \frac{1}{2\pi} \log(kR_0) \, T \right\| \to 0 \tag{2.31}$$

as $k \to 0$ where T is the finite-rank integral operator defined by

$$T\phi(x) = \int_\Gamma \phi(y) ds(y), \quad x \in \Gamma.$$

The following limiting behaviour of $A_{k,\eta}$ is clear from (2.30) and (2.31).

LEMMA 2.9. *As $k \to 0$,*

$$A_{k,\eta} = I + D_0 - i\eta S_0 (1 + o(1))$$

in 3D, while

$$A_{k,\eta} = I + D_0 + i\eta \frac{1}{2\pi} \log(kR_0) \, T - i\eta S_0 (1 + o(1))$$

in 2D. Thus, unless

$$\eta = \left\{ \begin{array}{ll} O(1), & d = 3, \\ O((\log k)^{-1}), & d = 2, \end{array} \right. \quad as \; k \to 0,$$

it holds that $\|A_{k,\eta}\| \to \infty$ as $k \to 0$. On the other hand, if, for some $c_0 \in \mathbb{R}$,

$$\eta \to c_0 \quad as \; k \to 0, \tag{2.32}$$

in the case $d = 3$ or

$$\eta \frac{1}{2\pi} \log(kR_0) \to c_0 \quad as \; k \to 0, \tag{2.33}$$

in the case $d = 2$, then

$$\|A_{k,\eta} - A_0\| \to 0 \quad as \; k \to 0,$$

where

$$A_0 := \left\{ \begin{array}{ll} I + D_0 - ic_0 S_0, & d = 3, \\ I + D_0 + ic_0 T, & d = 2. \end{array} \right.$$

The above lemma, coupled with the following theorem, makes clear that it is appropriate to choose η for low k so as to satisfy (2.32) or (2.33), for $d = 3, 2$, choosing $c_0 \neq 0$ in each case. This choice of η ensures that cond $A_{k,\eta}$ remains bounded in the limit as $k \to 0$. Clearly, one such choice of η is (2.29).

THEOREM 2.10. *Where A_0 is as defined in Lemma 2.9, it holds that, for $c_0 \neq 0$, A_0 is invertible as an operator on $H^s(\Gamma)$ for $0 \leq s \leq 1$, in particular as an operator on $L^2(\Gamma)$, while A_0 is not invertible for $c_0 = 0$. Thus, if (2.32) or (2.33) hold in the cases $d = 3$ and $d = 2$, respectively, then, as $k \to 0$, $\|A_{k,\eta}^{-1}\| = O(1)$, if $c_0 \neq 0$, while $\|A_{k,\eta}^{-1}\| \to \infty$, if $c_0 = 0$.*

Proof. The last sentence follows immediately from standard operator perturbation results and (2.33) and (2.32) once the first sentence is proved. In the case $c_0 = 0$ it

14

is well known that A_0 is not injective, having a non-trivial null space which is the set of constant functions, see e.g. [22, Theorem 6.20], [31]. To show invertibility of A_0 for $c_0 \neq 0$ we note first that, by interpolation, it is enough to show invertibility on $H^s(\Gamma)$ for $s = 0$ and 1 [26]. Further, since the difference $A_0 - A_{k,\eta}$ is a compact operator on $L^2(\Gamma)$ and on $H^1(\Gamma)$ (see e.g. the proof of Theorem 2.7 in [9]) and since $A_{k,\eta}$ is invertible, it holds that A_0 is Fredholm of index zero on $L^2(\Gamma)$ and on $H^1(\Gamma)$, so that it is invertible if and only if it is injective. Moreover, since A_0 is Fredholm with the same index on $H^1(\Gamma)$ and $L^2(\Gamma)$, and $L^2(\Gamma)$ is dense in $H^1(\Gamma)$, it follows from a standard result on Fredholm operators (see e.g. [28, §1]), that the null-space of A_0 is a subset of $H^1(\Gamma) \supset H^{1/2}(\Gamma)$. In the case that Γ is C^2 that there are no non-trivial functions in the null-space of A_0 in $C(\Gamma)$ is shown in [22, Theorem 6.24] in the case $d = 2$ and in [12, Theorem 3.33] in the case $d = 3$. In the case when Γ is Lipschitz the same arguments can be used to prove injectivity of A_0 in $H^{1/2}(\Gamma)$, replacing the mapping properties of layer potentials in classical function spaces in [12, 22] with those in Sobolev spaces in [26] (cf. the proof of Theorem 2.5 in [9]). $\square$

2.7. Bounds on condition numbers and choice of η. In this section we bring together the results from the sections above and explore their implications for the conditioning of $A_{k,\eta}$, and what this then implies regarding the choice of η to minimise cond $A_{k,\eta}$. We have already noted in §2.2 and §2.6 recommendations made in the literature regarding the choice of η, mainly based on study of the case when Γ is a circle or sphere. Overwhelmingly (see e.g. [20, 21, 3, 4, 17, 7, 8, 15]) the guidance is to take η proportional to k for all but small values of k. The choice of η for small k has been discussed already in §2.6. One choice of η, recommended by Kress [20] for the 3D case, that we have studied in §2.2, is $\eta = \max(1/(2R_0), k)$. This choice, by Lemma 2.9 above, is not suitable in the 2D case for low k, since with this choice $\|A_{k,\eta}\| \to \infty$ as $k \to 0$. An alternative choice, which satisfies (2.33) with $c_0 \neq 0$, and which we will use for computations in §4, is

$$\eta := \begin{cases} (R_0(1 - \log(kR_0)))^{-1}, & 0 < kR_0 \leq 1, \\ k, & kR_0 \geq 1. \end{cases} \tag{2.34}$$

Here R_0 is a length scale of the scatterer Ω; we choose R_0 as defined in §2.2 in §4. The following theorem, which follows from (2.6), (2.9), (2.12), (2.16), and Theorem 2.10, is a sharpening of results in [10, Section 6].

THEOREM 2.11. *Suppose that Γ is piecewise C^2 and starlike, in the sense of §2.2, and that η is given by (2.8) in the case $d = 3$, by (2.34) in the case $d = 2$. Then, for some constant $C \geq 1$,*

$$1 \leq \|A_{k,\eta}^{-1}\| \leq C, \quad 1 \leq \|A_{k,\eta}\| \leq C(1 + k^{(d-1)/2}),$$

so that

$$\text{cond } A_{k,\eta} \leq C^2(1 + k^{(d-1)/2})$$

for all $k > 0$. In the case $d = 2$ we have a sharper lower bound for k large, so that, for some $c > 1$,

$$c^{-1}(1 + k^{1/3}) \leq \text{cond } A_{k,\eta} \leq c(1 + k^{1/2}), \tag{2.35}$$

for $k > 0$.

For the case of a circle or sphere we saw in §2.1 that the above upper bounds are not sharp; with the proposed choices of η the sharper bound holds that

$$\text{cond } A_{k,\eta} \leq C(1 + k^{1/3}).$$

We will investigate, in the 2D case, which of the bounds in (2.35) is sharp in §4. We will also investigate the alternative choice for η for large k proposed in [5], namely to take $|\eta| = k^{2/3}$. It follows from (2.5) and (2.6) that, when Γ is a sphere, this choice of η also implies

$$\text{cond } A_{k,\eta} \leq C k^{1/3} \quad \text{for } k \geq 1.$$

We will explore whether this estimate holds for 2D geometries in §4. Note that for starlike polygons and the choices of η indicated in Theorem 2.11, it follows from Theorem 2.2 that, for some $c > 1$,

$$c^{-1}(1 + k^{1/2}) \leq \text{cond } A_{k,\eta} \leq c(1 + k^{1/2}),$$

for $k > 0$, i.e. it is the upper bound in (2.35) that is sharp in this case. We will illustrate this in the numerical results in §4.

For trapping obstacles, in the sense defined in §2.5, faster rates of growth of cond $A_{k,\eta}$ are inevitable. The following result is deduced in [10], by combining Theorems 2.2 and 2.7.

THEOREM 2.12. *[10, equation (6.13)] Suppose that the conditions of Theorem 2.7 are satisfied. Then, for some $C > 0$, where k_m is as defined in Theorem 2.7,*

$$\text{cond } A_{k_m,\eta} \geq C \, k_m^{9/10} \left(1 + |\eta|(1 + k_m)^{-1/2}\right) \left(1 + \frac{|\eta|}{k_m}\right)^{-1}, \quad m \in \mathbb{N}.$$

Thus, if $\eta = c(1 + k_m^p)$, for some constants c and p, then, for some constant $\tilde{C} > 0$,

$$\text{cond } A_{k_m,\eta} \geq \tilde{C}(1 + k_m^q), \quad m \in \mathbb{N},$$

with $q = 9/10$ for $0 \leq p \leq 1/2$, $q = p + 4/10$, for $1/2 \leq p \leq 1$, and $q = 14/10$ for $p \geq 1$.

For trapping obstacles satisfying the conditions of Theorem 2.8 the situation with regard to conditioning is much worse: the condition number must grow exponentially as k increases through some sequence of wavenumbers.

THEOREM 2.13. *Suppose that the conditions of Theorem 2.8 are satisfied. Then there exists a sequence $0 < k_0 < k_1 < k_2 < \ldots$, with $k_m \to \infty$ as $m \to \infty$, such that, for some $\gamma > 0$ and $C > 0$,*

$$\text{cond } A_{k_m,\eta} \geq C e^{\gamma k_m},$$

for $\eta \in \mathbb{R} \setminus \{0\}$ and $m = 0, 1, 2, \ldots$.

Proof. By Lemma 2.1 and Theorems 2.3 and 2.8, there exists a sequence $0 < k_0 < k_1 < k_2 < \ldots$, with $k_m \to \infty$ as $m \to \infty$, such that, for some $\gamma > 0$ and $C > 0$,

$$\text{cond } A_{k_m,\eta} \geq C \min\left(1, |\eta| k_m^{-2/3}\right) e^{\gamma k_m} \left(1 + \frac{|\eta|}{k_m}\right)^{-1}.$$

But for $|\eta| \leq k_m$ this implies that cond $A_{k_m,\eta} \geq \frac{1}{2} C e^{\gamma k_m}$ while for $|\eta| \geq k_m$ this implies that cond $A_{k_m,\eta} \geq \frac{1}{2} C k_m^{2/3} e^{\gamma k_m}$, and the result follows. $\square$

3. Discrete level. In this section we explore the relationship between $\|A_{k,\eta}\|$ and $\|A_{k,\eta}^{-1}\|$ and the norms of discrete versions of these operators, specifically the norms of matrices arising from Galerkin discretisations.

Let $X_N \subset L^2(\Gamma)$ be a finite-dimensional subspace with $P_N : L^2(\Gamma) \to X_N$ the corresponding orthogonal projection. Let V be a bounded linear operator on $L^2(\Gamma)$. Then, given $y \in L^2(\Gamma)$, a Galerkin method for solving the equation

$$V x = y$$

for $x \in L^2(\Gamma)$, is to seek $x_N \in X_N$ such that

$$P_N V x_N = P_N y. \tag{3.1}$$

Let $\{\phi_1, \dots, \phi_N\}$ be an orthonormal basis of X_N, define $V_N : X_N \to X_N$ by $V_N := P_N V|_{X_N}$, and let $T_N : X_N \to \mathbb{C}^N$ be defined by

$$T_N x = [(x, \phi_1) \cdots (x, \phi_N)]^T.$$

Then T_N is an isomorphism, indeed an isometric isomorphism if we give $\mathbb{C}^N$ the standard Euclidean norm $\| \cdot \|_2$. Further (3.1) is equivalent to

$$V^N T_N x_N = T_N P_N y,$$

where

$$V^N := T_N V_N T_N^{-1}$$

is the linear operator on $\mathbb{C}^N$ whose matrix representation (that we denote also by V^N) is the Galerkin matrix $V^N = [(V\phi_j, \phi_i)]$. Clearly

$$\|V_N\| = \|V^N\| \tag{3.2}$$

(where we use $\| \cdot \|$ on the right hand side to denote the matrix norm induced by the vector norm $\| \cdot \|_2$), since both T_N and T_N^{-1} are isometries. Also V_N is invertible if and only if V^N is invertible and, if they are both invertible, then

$$\|V_N^{-1}\| = \|(V^N)^{-1}\|.$$

Now we need to determine the relationship between $\|V_N\|$ and $\|V\|$. We first require the following result.

LEMMA 3.1. *If W is a bounded linear operator on $L^2(\Gamma)$ and $P_1, P_2, \dots$ is a sequence of orthogonal projection operators with $P_N \phi \to \phi$ for all $\phi \in L^2(\Gamma)$, then*

$$\|P_N W P_N\| \to \|W\|,$$

as $N \to \infty$.

Proof. Let $\lambda = \liminf_{N \to \infty} \|P_N W P_N\|$ and choose a monotonic increasing sequence $N_1, N_2, \dots$ of natural numbers with $\|P_{N_k} W P_{N_k}\| \to \lambda$ as $k \to \infty$. Then, for every $\phi \in L^2(\Gamma)$,

$$\|W\phi\| = \lim_{k \to \infty} \|P_{N_k} W P_{N_k} \phi\| \le \lim_{k \to \infty} \|P_{N_k} W P_{N_k}\| \|\phi\| = \lambda \|\phi\|,$$

and hence $\|W\| \le \lambda = \liminf_{N \to \infty} \|P_N W P_N\|$. On the other hand, we have

$$\limsup_{N \to \infty} \|P_N W P_N\| \le \|W\|,$$

17

since $\|P_N W P_N\| \leq \|P_N\| \|W\| \|P_N\| = \|W\|$ for every N, and hence

$$\|W\| \leq \liminf_{N \to \infty} \|P_N W P_N\| \leq \limsup_{N \to \infty} \|P_N W P_N\| \leq \|W\|.$$

Thus $\lim_{N \to \infty} \|P_N W P_N\|$ exists and is equal to $\|W\|$. $\square$

Clearly $\|P_N V P_N\| = \|V_N\|$, so that it follows from (3.2) and Lemma 3.1 that

$$\|V^N\| = \|V_N\| = \|P_N V P_N\| \to \|V\|, \qquad (3.3)$$

as $N \to \infty$.

In the case that $V = I + C$ with C compact, it holds moreover that $\|(V^N)^{-1}\| \to \|V^{-1}\|$ as $N \to \infty$ if V is invertible. To see this, note first that, by Lemma 3.1, if V is invertible,

$$\|P_N V^{-1} P_N\| \to \|V^{-1}\|,$$

as $N \to \infty$. Next, let $\tilde{V}_N = I + P_N C$ and note that

$$V_N = \tilde{V}_N|_{X_N},$$

and that, since P_N converges strongly (i.e. pointwise) to the identity and C is compact, $P_N C$ converges in norm to C, so that $\|V - \tilde{V}_N\| \to 0$. It follows from standard operator convergence results that $\tilde{V}_N$ is invertible for all sufficiently large N. But then it follows that also $V_N = \tilde{V}_N|_{X_N}$ is invertible (as an operator on X_N). Indeed, injectivity of V_N is clear by injectivity of $\tilde{V}_N$. To see surjectivity, take $\psi \in X_N$ and note that, by surjectivity of $\tilde{V}_N$, there exists a $\phi \in L^2(\Gamma)$ with $\psi = \tilde{V}_N \phi = \phi + P_N C \phi$, so that $\phi = \psi - P_N C \phi \in X_N$ and hence, $V_N \phi = \psi$. This argument also shows that $V_N^{-1} = \tilde{V}_N^{-1}|_{X_N}$. Further, $\|\tilde{V}_N^{-1} - V^{-1}\| \to 0$ as $N \to \infty$, so that

$$\begin{aligned}
\|P_N V^{-1} P_N - P_N \tilde{V}_N^{-1} P_N\| &= \|P_N(V^{-1} - \tilde{V}_N^{-1})P_N\| \\
&\leq \|P_N\| \|V^{-1} - \tilde{V}_N^{-1}\| \|P_N\| \\
&= \|V^{-1} - \tilde{V}_N^{-1}\| \to 0,
\end{aligned}$$

as $N \to \infty$. Hence, as $N \to \infty$,

$$\|(V^N)^{-1}\| = \|V_N^{-1}\| = \|P_N \tilde{V}_N^{-1} P_N\| = \|P_N V^{-1} P_N\| + o(1) \to \|V^{-1}\|. \qquad (3.4)$$

Equation (3.3) applies to the Galerkin boundary element method discretisation of all the operators we have discussed in the previous sections, in particular to S_k, D_k, and $A_{k,\eta}$, provided that the sequence of approximation spaces X_N is chosen so that P_N converges pointwise to the identity. It is enough to check that this pointwise convergence holds on some dense subset, for example to check that

$$\|P_N \phi - \phi\| = \inf_{\phi_N \in X_N} \|\phi_N - \phi\| \to 0 \text{ as } N \to \infty, \quad \text{for every } \phi \in C(\Gamma).$$

Equation (3.4) applies to the operator $A_{k,\eta}$ if Γ is C^1, for then $A_{k,\eta}$ has the form $A_{k,\eta} = I + C_{k,\eta}$ with $C_{k,\eta}$ compact [16]. For general Lipschitz Γ, it is not known whether (3.4) holds, indeed it is not even known for any Galerkin method that V^N is invertible for all sufficiently large N.

4. Numerical results. In this section we compute $\|V^N\|$ for $V = S_k, D_k, A_{k,\eta}$, and $\|(V^N)^{-1}\|$ for $V = A_{k,\eta}$, each for a variety of obstacles, and we compare the computed values with the upper and lower bounds on the corresponding continuous operators as described in §2. The aim is to provide supporting evidence for some of the theoretical results described in §2, both quantitative and asymptotic, and to give some indication of which of the upper and lower bounds may be sharper, particularly when there is a significant gap between them. We also seek an indication of the extent to which the bounds on the continuous operators are satisfied by their discrete counterparts.

We present results for $\eta = k$ for all geometries under consideration, and we also present results for $\eta = k^{2/3}$ for certain specific examples. As we have discussed in §2.7, the choice $\eta = k$ is widespread in the literature, e.g. [3, 4, 15, 17, 20], and this choice is supported by our own preceding analysis. The interesting choice $\eta = k^{2/3}$, proposed in [5], is also supported by some of the above analysis; for example we have seen in §2.7 that, for a spherical scatterer, cond $A_{k,\eta}$ increases at the same rate as $k \to \infty$ whether η is proportional to k or proportional to $k^{2/3}$.

Although our main focus is on larger values of k, for two examples we also investigate the limit $k \to 0$, presenting results for $\eta = k$ and for η given by (2.34).

In each example the boundary Γ is piecewise C^∞, that is $\Gamma = \bigcup_{j=1}^p \Gamma^{(j)}$ with $\Gamma^{(j)}$ a C^∞ arc. We denote the length of $\Gamma^{(j)}$ by L_j, and divide each $\Gamma^{(j)}$ into N_j segments $\Gamma_i^{(j)}$, $i = 1, \ldots, N_j$ of equal length $|\Gamma_i^{(j)}| = L_j/N_j$. We then define the orthonormal basis functions by

$$\tilde{\phi}_i^{(j)}(x) = \begin{cases} 1/|\Gamma_i^{(j)}|^{1/2}, & x \in \Gamma_i^{(j)}, \\ 0, & \text{otherwise,} \end{cases} \quad i = 1, \ldots, N_j.$$

Now whilst in theory $\|V\| = \lim_{N \to \infty} \|V^N\|$, in practice we can only compute $\|V^N\|$ for a finite value of N. In order to justify the assumption that our choice of N_j is sufficiently large we fix $N_j \propto k$, choosing the constant of proportionality on the basis of some simple model experiments. In particular, for the case that Ω is a circle the eigenvalues of $A_{k,\eta}$ are known explicitly, with corresponding formulae in terms of the eigenvalues for $\|A_{k,\eta}\|$ and $\|A_{k,\eta}^{-1}\|$ (see [10, §2] for details). Thus for a circle we can compare our computed approximations to $\|A_{k,\eta}\|$ and $\|A_{k,\eta}^{-1}\|$ with the known values. For this example we found that ten basis functions per wavelength gives a relative error of approximately 1%, and thus in each example we choose $N_j \approx \frac{10kL_j}{2\pi}$.

We present numerical results for the obstacles shown in Figure 4.1. More detailed descriptions of the obstacles are provided below. For each obstacle and for each operator V_k we also compute the algebraic growth rate p under the assumption that $\|V_k\| = Ck^p$, for some constant $C > 0$. Assuming this formula holds, we can estimate the value of p from two successive values $\|V_{k_j}\|$ and $\|V_{k_{j+1}}\|$ by

$$p = \frac{\log\left(\frac{\|V_{k_{j+1}}\|}{\|V_{k_j}\|}\right)}{\log\left(\frac{k_{j+1}}{k_j}\right)}. \tag{4.1}$$

In the cases where $p \approx 0$, p is not shown in the tables. In all of the estimates detailed below, C and C_j, $j = 1, 2, \ldots$, denote unspecified constants independent of k and η.

4.1. Circle. For our first example, we consider the unit circle. From (2.17) and (2.3) we know that, for $k \geq 1$

$$(32\pi)^{-1/3} k^{-2/3}(1 + o(1)) \leq \|S_k\| \leq Ck^{-2/3},$$

19

Circle · Ellipse · Kite · Crack · Square · Thin Rectangle · Rectangular cavity · Elliptic Cavity
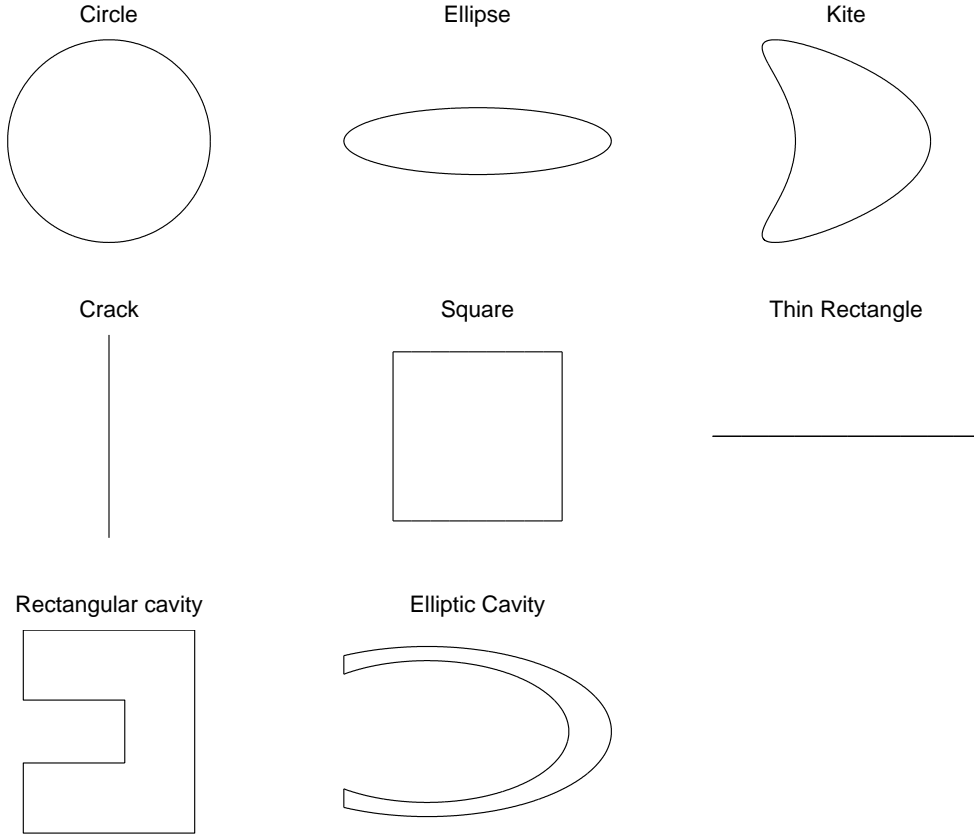
FIG. 4.1. *Obstacles corresponding to numerical experiments.*

where here and throughout this section $o(1)$ denotes a term which vanishes in the limit as $k \to \infty$. Theorem 2.6, (2.3) and (2.11) imply that, for $k > 0$,

$$C_1 \le \|D_k\| \le C_2 k^{1/2} + C_3,$$

whilst we know that the sharper upper bound (2.4) holds in the case of a sphere, that $\|D_k\| \le C$. The numerical results in Table 4.1 for the corresponding boundary element matrices suggest that this sharper result, proved for a sphere, appears to be applicable for a circle as well; we observe for the discrete approximations that $\|S_k\| \sim k^{-2/3}$ and $\|D_k\| \sim k^0$ ($\sim$ in this section indicates that the ratio of the left hand side to the right hand side is approximately constant in the limit $k \to \infty$). The quantitative lower bound on $\|S_k\|$ from (2.17) is clearly a lower bound in Table 4.1, underestimating the true norm by a factor of about 6.5.

From Lemma 2.1, Corollary 2.4, (2.1) and (2.12) we know that, for $k \ge 1$,

$$\left(\frac{k}{32\pi}\right)^{1/3} (1 + o(1)) \le \|A_{k,k}\| \le C_1 k^{1/3},$$

$$1 \le \|A_{k,k^{2/3}}\| \le C_2 k^{1/2}.$$

Note that Corollary 2.4 gives the lower bound $(32\pi)^{-1/3} - 1/(2\sqrt{2}) \approx -0.139$ on $\|A_{k,k^{2/3}}\|$, as $k \to \infty$, which is clearly less sharp than the lower bound on $\|A_{k,k^{2/3}}\|$

k	$(32\pi)^{-1/3}k^{-2/3}$	$\|S_k\|$	p	$\|D_k\|$
5	7.355×10^{-2}	5.240×10^{-1}		1.144
10	4.633×10^{-2}	3.152×10^{-1}	-0.73	1.114
20	2.919×10^{-2}	1.997×10^{-1}	-0.66	1.084
40	1.839×10^{-2}	1.246×10^{-1}	-0.68	1.079
80	1.158×10^{-2}	7.798×10^{-2}	-0.68	1.076
160	7.297×10^{-3}	4.884×10^{-2}	-0.68	1.075
320	4.597×10^{-3}	3.076×10^{-2}	-0.67	1.072
640	2.896×10^{-3}	1.935×10^{-2}	-0.67	1.071

TABLE 4.1

Circle. *Norms of Galerkin BEM approximations to S_k and D_k, and p values given by (4.1).*

from Lemma 2.1. The upper bound on $\|A_{k,k^{2/3}}\|$ for the case of a sphere is, from (2.5), $\|A_{k,k^{2/3}}\| \leq C_3$. The numerical results in Table 4.2 suggest that this sharper result also holds for a circle; the results suggest $\|A_{k,k^{2/3}}\| \sim k^0$, and that $\|A_{k,k}\| \sim k^{1/3}$ as expected. The quantitative lower bound on $\|A_{k,k}\|$ from Corollary 2.4 is a lower bound in Table 4.2, underestimating the true norm by a factor of about 7.

k	$\left(\frac{k}{32\pi}\right)^{1/3}$	$\|A_{k,k}\|$	p	$\|A^{-1}_{k,k}\|$	$\|A_{k,k^{2/3}}\|$	$\|A^{-1}_{k,k^{2/3}}\|$	p	$B_{0,k^{2/3}}$
5	0.37	2.663		0.986	2.016	0.995		3.82
10	0.46	3.233	0.28	0.987	1.993	1.056	0.09	4.49
20	0.58	4.021	0.32	0.987	1.981	1.260	0.26	5.38
40	0.74	5.030	0.32	0.987	2.000	1.701	0.43	6.56
80	0.93	6.271	0.32	0.987	1.999	2.039	0.26	8.06
160	1.17	7.859	0.33	0.987	1.990	2.694	0.40	9.98
320	1.47	9.883	0.33	0.987	1.998	3.407	0.34	12.40
640	1.85	12.419	0.33	0.987	2.000	4.307	0.34	15.49

TABLE 4.2

Circle. *Galerkin BEM approximations to $\|A_{k,\eta}\|$ and $\|A^{-1}_{k,\eta}\|$.*

By Lemma 2.1, $\|A^{-1}_{k,k}\| \geq 1$, which combined with (2.2) implies that $\|A^{-1}_{k,k}\| = 1$ for all k sufficiently large, and the numerical results in Table 4.2 show this behaviour. The bound for general starlike obstacles applied to the circle, i.e. (2.7), gives that

$$\|A^{-1}_{k,\eta}\| \leq \frac{1}{2} + \left[1 + \frac{k^2}{\eta^2} + \frac{(1+2k)^2}{2\eta^2}\right]^{1/2} =: B_{0,\eta}.$$

Note that $B_{0,k} \to 2.5$ (in fact it holds that $2.5 \leq B_{0,k} \leq 2.6$ for the range of k in Table 4.2), and that $B_{0,k^{2/3}} \sim \sqrt{3}\,k^{1/3}$ as $k \to \infty$. We see from Table 4.2 that $B_{0,\eta}$ appears to be an upper bound for the discretisation of $\|A^{-1}_{k,\eta}\|$ as predicted, overestimatimating by a factor of about 2.5 for the larger values of k when $\eta = k$, by a factor of about 3.6 when $\eta = k^{2/3}$.

We note from Table 4.2 that, for this example, the condition number cond $A_{k,\eta} = \|A_{k,\eta}\|\,\|A^{-1}_{k,\eta}\|$ appears to be slightly numerically smaller for $\eta = k^{2/3}$ than for $\eta = k$. It appears that, for both choices of η, cond $A_{k,\eta}$ increases approximately in proportion to $k^{1/3}$, though this is less clear in the case $\eta = k^{2/3}$.

4.2. Ellipse. Next we consider the ellipse given by $(2\cos t, \frac{1}{2}\sin t)$, $t \in [0, 2\pi]$. The more specific results of §2.1 do not apply in this case, and for upper bounds

21

on $\|S_k\|$ and $\|D_k\|$ we have only the results for general Lipschitz Γ of §2.3. The inequalities (2.17) and (2.10) imply that, for $k \geq 1$,

$$(4\pi)^{-1/3} k^{-2/3}(1 + o(1)) \leq \|S_k\| \leq Ck^{-1/2},$$

the lower bound larger than for the case of the circle as the maximum radius of curvature ($R = 8$) is larger. Theorem 2.6 and (2.11) with $N = 0$ imply that, for $k > 0$,

$$C_1 \leq \|D_k\| \leq C_2 k^{1/2} + C_3.$$

Inspecting the numerical results in Table 4.3, we see that the quantitative lower bound on $\|S_k\|$ from (2.17) is clearly a lower bound for the norm of the discretised operator, underestimating the true norm by a factor of about 6 at the highest wavenumbers (cf. the results for the circle). The numerical results for $\|D_k\|$ suggest that $\|D_k\| \sim k^0$, i.e. that the lower bound on $\|D_k\|$ is sharp, while it appears from the numerical results that $\|S_k\| \sim k^p$, for $p \approx -0.6$.

k	$(4\pi)^{-1/3} k^{-2/3}$	$\|S_k\|$	p	$\|D_k\|$	p
5	1.471×10^{-1}	6.692×10^{-1}		1.458	
10	9.267×10^{-2}	4.143×10^{-1}	-0.69	1.591	0.13
20	5.838×10^{-2}	2.730×10^{-1}	-0.60	1.671	0.07
40	3.678×10^{-2}	1.803×10^{-1}	-0.60	1.760	0.08
80	2.317×10^{-2}	1.209×10^{-1}	-0.58	1.819	0.05
160	1.459×10^{-2}	8.029×10^{-2}	-0.59	1.877	0.05
320	9.194×10^{-3}	5.269×10^{-2}	-0.61	1.919	0.03
640	5.792×10^{-3}	3.427×10^{-2}	-0.62	1.942	0.02

TABLE 4.3
Ellipse. *Galerkin BEM approximations to* $\|S_k\|$ *and* $\|D_k\|$.

Now turning to Table 4.4, note that Lemma 2.1, Corollary 2.4 and (2.12) imply that, for $k \geq 1$,

$$\left(\frac{k}{4\pi}\right)^{1/3}(1 + o(1)) \leq \|A_{k,k}\| \leq C_1 k^{1/2},$$

$$1 \leq \|A_{k,k^{2/3}}\| \leq C_2 k^{1/2}. \tag{4.2}$$

(Note that Corollary 2.4 gives the lower bound $(4\pi)^{-1/3} - 1/(2\sqrt{2}) \approx 0.077$ on $\|A_{k,k^{2/3}}\|$, as $k \to \infty$. So in (4.2) we have used the sharper estimate from Lemma 2.1.) The numerical results in Table 4.4 suggest that $\|A_{k,k}\| \sim k^p$ for $p \approx 0.4$, that $\|A_{k,k^{2/3}}\| \sim k^0$, and that the lower bound in (4.2) is an underestimate by a factor approximately 2.5.

Lemma 2.1 and (2.6) imply that, for $k \geq 1$,

$$1 \leq \|A_{k,k}^{-1}\| \leq C_1, \quad 1 \leq \|A_{k,k^{2/3}}^{-1}\| \leq C_2 k^{1/3}. \tag{4.3}$$

The numerical results in Table 4.4 suggest that $\|A_{k,k}^{-1}\| \approx 1$ for $k \geq 5$. The values of p corresponding to $\|A_{k,k^{2/3}}^{-1}\|$ are rather variable, but the average of the last six values for p is 0.34, approximately consistent with the upper bound $C_2 k^{1/3}$.

As for the case of the circle the condition number cond $A_{k,\eta} = \|A_{k,\eta}\| \|A_{k,\eta}^{-1}\|$ appears to be numerically smaller for $\eta = k^{2/3}$ than for $\eta = k$, by nearly a factor 2 for the higher values of k in Table 4.4.

k	$\left(\frac{k}{4\pi}\right)^{1/3}$	$\|A_{k,k}\|$	p	$\|A_{k,k}^{-1}\|$	$\|A_{k,k^{2/3}}\|$	$\|A_{k,k^{2/3}}^{-1}\|$	p
5	0.736	3.507		0.987	2.417	0.996	
10	0.927	4.267	0.28	0.987	2.473	1.024	0.04
20	1.168	5.589	0.39	0.987	2.554	1.300	0.34
40	1.471	7.317	0.39	0.987	2.599	1.662	0.35
80	1.853	9.751	0.41	0.987	2.580	1.986	0.26
160	2.335	12.902	0.40	0.987	2.582	2.548	0.36
320	2.942	16.906	0.39	0.987	2.634	3.387	0.41
640	3.707	21.972	0.38	0.987	2.689	4.287	0.34

<div align="center">TABLE 4.4</div>

Ellipse. *Galerkin BEM approximations to $\|A_{k,\eta}\|$ and $\|A_{k,\eta}^{-1}\|$.*
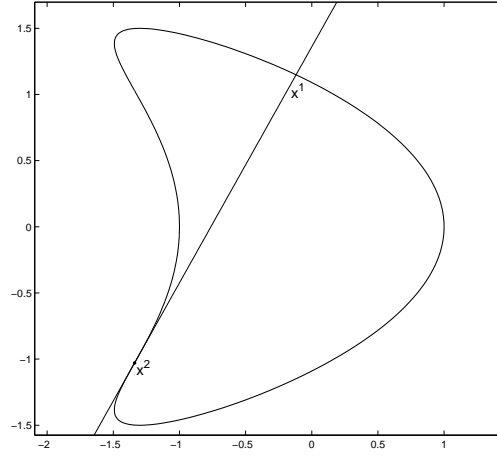

<div align="center">FIG. 4.2. *The 'kite' shape and notation of §4.3.*</div>

4.3. Kite. Estimates for $\|S_k\|$, $\|D_k\|$, $\|A_{k,k}\|$, $\|A_{k,k}^{-1}\|$, $\|A_{k,k^{2/3}}\|$ and $\|A_{k,k^{2/3}}^{-1}\|$ for the 'kite' shape given by $(\cos t + 0.65\cos 2t - 0.65, 1.5\sin t)$, $t \in [0, 2\pi]$, are shown in Tables 4.5 and 4.6, for various k. Our upper bounds from §2 that apply in this case are identical in their dependence on k to those for the ellipse. However, in contrast to the circle and the ellipse, our lower bounds imply significant growth in $\|D_k\|$ and $\|A_{k,k^{2/3}}\|$ as k increases. Specifically, applying Theorem 2.3 to the non-convex kite, with $N = 2$ and x^* the point of inflection on Γ labelled x^2 in Figure 4.2, and recalling (2.10) and (2.12), it follows that, for $k \geq 1$,

$$
\begin{aligned}
C_1 k^{-3/5} &\leq \|S_k\| \leq C_2 k^{-1/2}, \\
C_1 k^{2/5} &\leq \|A_{k,k}\| \leq C_2 k^{1/2}, \\
C_1 k^{1/15} &\leq \|A_{k,k^{2/3}}\| \leq C_2 k^{1/2}.
\end{aligned}
$$

Moreover, applying Theorem 2.6 to the non-convex kite, with $N = 2$, x^2 one of the points of inflection on Γ, and x^1 the other point on Γ intersected by the tangent at

<div align="center">23</div>

x^2 (see Figure 4.2), and recalling (2.11), we have, for $k \geq 1$,

$$C_1 k^{1/6} \leq \|D_k\| \leq C_2 k^{1/2}.$$

The numerical results in Tables 4.5 and 4.6 provide some support for these estimates. The lower bound on $\|S_k\|$ seems sharper than the upper bound, although in fact the behaviour of $\|S_k\|$ appears to be rather similar to that for the ellipse. On the other hand, the behaviour of $\|D_k\|$ and $\|A_{k,k^{2/3}}\|$ is very different from that seen for the ellipse, with, approximately, $\|D_k\| \sim k^{1/4}$ and $\|A_{k,k^{2/3}}\| \sim k^{1/6}$.

Since the kite shape is starlike, satisfying the assumptions of §2.2, the same bounds (4.3) hold on $\|A_{k,k}^{-1}\|$ and $\|A_{k,k^{2/3}}^{-1}\|$ as for the case of the ellipse. We observe similar behaviour to that of the ellipse, namely that $\|A_{k,k}^{-1}\| \approx 1$ and that the bound $\|A_{k,k^{2/3}}^{-1}\| \leq C_2 k^{1/3}$ appears sharp. In Table 4.6 cond $A_{k,k^{2/3}} \sim k^p$, with $p \approx 0.47$, a faster rate of growth than cond $A_{k,k} \sim k^{1/3}$, so that, for the larger values of k, cond $A_{k,k} <$ cond $A_{k,k^{2/3}}$.

k	$\|S_k\|$	p	$\|D_k\|$	p
5	6.591×10^{-1}		1.810	
10	4.365×10^{-1}	-0.59	2.169	0.27
20	2.758×10^{-1}	-0.63	2.686	0.29
40	1.712×10^{-1}	-0.65	3.160	0.27
80	1.074×10^{-1}	-0.65	3.616	0.25
160	6.759×10^{-2}	-0.66	4.160	0.24
320	4.400×10^{-2}	-0.65	4.760	0.24
640	2.866×10^{-2}	-0.65	5.437	0.23

TABLE 4.5
Kite. *Galerkin BEM approximations to $\|S_k\|$ and $\|D_k\|$.*

k	$\|A_{k,k}\|$	p	$\|A_{k,k}^{-1}\|$	$\|A_{k,k^{2/3}}\|$	p	$\|A_{k,k^{2/3}}^{-1}\|$	p
5	3.720		0.987	2.764		1.029	
10	4.766	0.36	0.987	3.243	0.23	1.027	0
20	6.151	0.37	0.987	3.602	0.15	1.177	0.20
40	7.513	0.29	0.987	4.041	0.17	1.511	0.36
80	9.316	0.31	0.987	4.394	0.12	1.883	0.32
160	11.563	0.31	0.987	4.891	0.16	2.354	0.32
320	14.337	0.31	0.987	5.414	0.15	2.954	0.33
640	18.387	0.36	0.987	6.030	0.16	3.671	0.31

TABLE 4.6
Kite. *Galerkin BEM approximations to $\|A_{k,k}\|$, $\|A_{k,k}^{-1}\|$, $\|A_{k,k^{2/3}}\|$ and $\|A_{k,k^{2/3}}^{-1}\|$.*

4.4. Crack. This numerical example is distinct from the others in that Γ is an open arc, the straight line from $(0,0)$ to $(0,1)$, and the only theory which applies from §2 are the upper and lower bounds for $\|S_k\|$. Computations of the Galerkin BEM approximations to $\|S_k\|$ are shown in Table 4.7 for various k. From (2.13) and Theorem 2.2 it follows that

$$\frac{1}{\sqrt{\pi k}} + O(k^{-1}) \leq \|S_k\| \leq \frac{2}{\sqrt{\pi k}}. \tag{4.4}$$

The results in Table 4.7 clearly demonstrate that $\|S_k\| \sim k^{-1/2}$ (cf. [32]), a slower rate of decay than for the circle, ellipse or kite, and that the values of $\|S_k\|$ are bracketed between the quantitative upper and lower bounds in (4.4), nearly coinciding with the lower bound values.

k	$\|S_k\|$	p	$\sqrt{1/(\pi k)}$	$2\sqrt{1/(\pi k)}$
5	2.649×10^{-1}		2.523×10^{-1}	5.046×10^{-1}
10	1.817×10^{-1}	-0.54	1.784×10^{-1}	3.568×10^{-1}
20	1.266×10^{-1}	-0.52	1.262×10^{-1}	2.523×10^{-1}
40	8.960×10^{-2}	-0.50	8.921×10^{-2}	1.784×10^{-1}
80	6.326×10^{-2}	-0.52	6.308×10^{-2}	1.262×10^{-1}
160	4.472×10^{-2}	-0.50	4.460×10^{-2}	8.921×10^{-2}
320	3.162×10^{-2}	-0.50	3.154×10^{-2}	6.308×10^{-2}
640	2.236×10^{-2}	-0.50	2.230×10^{-2}	4.460×10^{-2}

TABLE 4.7
Crack. *Galerkin BEM approximations for $\|S_k\|$, and theoretical lower and upper bounds.*

4.5. Square. Computed estimates for $\|S_k\|$, $\|D_k\|$, $\|A_{k,k}\|$, $\|A_{k,k}^{-1}\|$, $\|A_{k,k^{2/3}}\|$ and $\|A_{k,k^{2/3}}^{-1}\|$ for the square of side length two are shown in Tables 4.8 and 4.9 below, for various k. The theoretical upper bounds from §2 that apply are identical to those for the ellipse and kite examples above. In particular, since the square is starlike satisfying the conditions of §2.2, the bounds (4.3) apply. However, as Γ now contains a straight line segment we have different lower bounds on $\|S_k\|$, $\|A_{k,\eta}\|$ and $\|D_k\|$ compared to the ellipse and the kite. Specifically, applying Theorem 2.2 and recalling (2.10) and (2.12), it follows that, for $k \geq 1$,

$$\sqrt{\frac{2}{\pi k}} + O(k^{-1}) \quad \leq \|S_k\| \leq \quad Ck^{-1/2}, \tag{4.5}$$

$$\sqrt{\frac{2k}{\pi}} - 1 + O(1) \quad \leq \|A_{k,k}\| \leq \quad Ck^{1/2}, \tag{4.6}$$

$$\sqrt{\frac{2}{\pi}}k^{1/6} - 1 + O(k^{-1/3}) \leq \|A_{k,k^{2/3}}\| \leq Ck^{1/2}. \tag{4.7}$$

Applying Theorem 2.5 and recalling (2.11), we also have

$$C_1 k^{1/4} \leq \|D_k\| \leq C_2 k^{1/2}. \tag{4.8}$$

It appears from Table 4.8 that $\|S_k\| \sim k^{-1/2}$, as expected, and the quantitative lower bound in (4.5) appears to be sharp, underestimating $\|S_k\|$ by only 3% at the highest frequency. It also seems that $\|D_k\| \sim k^{1/4}$, indicating that the lower bound in (4.8) is sharp in its dependence on k.

The results in Table 4.9 suggest that $\|A_{k,k}\| \sim k^p$, with $p \approx 1/2$, as expected from (4.6). It appears that $\|A_{k,k^{2/3}}\|$ is increasing roughly like $k^{1/5}$. The quantitative lower bound in (4.7) is seen to be a lower bound for the Galerkin BEM discretisation of $\|A_{k,k^{2/3}}\|$ in Table 4.9, underestimating $\|A_{k,k^{2/3}}\|$ by about a factor 3.5 at the highest frequency. As in the cases of the circle, ellipse, and kite, $\|A_{k,k}^{-1}\| \approx 1$ for all k, while $\|A_{k,k^{2/3}}^{-1}\|$ is increasing as k increases, though the rate of increase is somewhat erratic (from (2.6), we recall that $\|A_{k,k^{2/3}}^{-1}\| \leq Ck^{1/3}$). However, it appears that

k	$\sqrt{\frac{2}{\pi k}}$	$\|S_k\|$	p	$\|D_k\|$	p
5	3.568×10^{-1}	5.784×10^{-1}		1.316	
10	2.523×10^{-1}	3.353×10^{-1}	-0.79	1.488	0.18
20	1.784×10^{-1}	2.137×10^{-1}	-0.65	1.730	0.22
40	1.262×10^{-1}	1.428×10^{-1}	-0.58	2.018	0.22
80	8.921×10^{-2}	9.760×10^{-2}	-0.55	2.389	0.24
160	6.308×10^{-2}	6.723×10^{-2}	-0.54	2.825	0.24
320	4.460×10^{-2}	4.667×10^{-2}	-0.53	3.346	0.25
640	3.154×10^{-2}	3.259×10^{-2}	-0.52	3.972	0.25

TABLE 4.8

Square. *Galerkin BEM approximations for $\|S_k\|$ and $\|D_k\|$.*

cond $A_{k,k^{2/3}} \sim k^p$, with $p \approx 0.6$, a faster rate of growth than cond $A_{k,k} \sim k^{1/2}$, and, for the largest value of k, cond $A_{k,k} \approx$ cond $A_{k,k^{2/3}}$.

Where $R_0 > 0$ is some length scale of the scatterer, it follows from Theorem 2.11 that choosing

$$\eta = \eta^* := 1/(R_0(1 - \ln(kR_0))),$$

ensures $\|A_{k,\eta}\|$ and $\|A_{k,\eta}^{-1}\|$ remain bounded as $k \to 0$. This is true for any Lipschitz Γ and (rather arbitrarily) we choose this example to illustrate this numerically. Define R_0 as in §2.2, so $R_0 = \sqrt{2}$ for this particular scatterer (taking the origin at the centre of the square). With this choice of R_0, we show in Table 4.10 norm computations for small values of k. We see that, while $\|A_{k,k}^{-1}\|$ seems to blow up for small values of k, the values of $\|A_{k,\eta^*}^{-1}\|$ remain essentially constant, and cond A_{k,η^*} appears to be approaching a limit of about 3.7 as $k \to 0$. For the computations in Table 4.10, deviating from the element sizes used in the other calculations, we discretised each boundary line of the square with 500 equal length elements so as to be able to resolve the blow up in the norm of the inverse of $A_{k,k}$ with some accuracy.

k	$\|A_{k,k}\|$	p	$\|A_{k,k}^{-1}\|$	$\sqrt{\frac{2}{\pi}}k^{1/6}-1$	$\|A_{k,k^{2/3}}\|$	p	$\|A_{k,k^{2/3}}^{-1}\|$	p
5	3.089		1.024	0.043	2.237		1.116	
10	3.611	0.23	1.024	0.171	2.375	0.09	1.172	0.07
20	4.608	0.35	1.023	0.315	2.536	0.10	1.280	0.13
40	6.032	0.39	1.023	0.476	2.865	0.18	1.484	0.21
80	8.117	0.43	1.023	0.656	3.187	0.15	1.904	0.36
160	11.068	0.45	1.023	0.859	3.600	0.18	2.315	0.28
320	15.253	0.46	1.023	1.087	4.131	0.20	3.065	0.41
640	21.177	0.47	1.023	1.342	4.777	0.21	4.064	0.41

TABLE 4.9

Square. *Galerkin BEM approximations for $\|A_{k,k}\|$, $\|A_{k,k}^{-1}\|$, $\|A_{k,k^{2/3}}\|$ and $\|A_{k,k^{2/3}}^{-1}\|$.*

4.6. Thin rectangle. The bound (2.6) suggests that, even if the obstacle Ω is starlike, $\|A_{k,\eta}^{-1}\|$ may blow up as the obstacle becomes very thin when δ_+/δ_- is small. In this example we investigate the extent to which such a blow up happens. Where δ is the thickness of the scatterer, it is reasonable to expect this to be a problem when $k\delta \ll 1$, for if $\kappa(x,y)$, $x,y \in \Gamma$, denotes the kernel of the integral operator

k	$\|A_{k,k}\|$	$\|A_{k,k}^{-1}\|$	p	$\|A_{k,\eta^*}\|$	$\|A_{k,\eta^*}^{-1}\|$
10^{-5}	1.608	3684.85		1.738	2.106
10^{-4}	1.608	465.66	-0.89	1.723	2.105
10^{-3}	1.608	61.63	-0.88	1.703	2.104
10^{-2}	1.608	9.04	-0.83	1.680	2.100
10^{-1}	1.612	2.11	-0.63	1.693	2.081
1	2.391	1.88	-0.05	2.534	1.871

TABLE 4.10

Square. *Galerkin BEM approximations for* $\|A_{k,k}\|$, $\|A_{k,k}^{-1}\|$, $\|A_{k,\eta^*}\|$ *, and* $\|A_{k,\eta^*}^{-1}\|$.

$D_k - i\eta S_k$ and $x_\pm \in \Gamma$ are adjacent points on opposite sides of a thin part of Γ, then $\kappa(x_+, y) \approx \kappa(x_-, y)$, $y \in \Gamma$, so that the integral operator should be badly conditioned. To explore the extent to which this is a problem, and the extent to which the bound (2.6) reflects actual behaviour in this limit, we show estimates for $\|A_{k,k}\|$ and $\|A_{k,k}^{-1}\|$ for a rectangle with side lengths 2 and 0.02 in Table 4.11 below, for various small values of k.

Using the notation of §2.2, for this example we have $\delta^* = \delta^+ = 2$, $\delta_- = 0.02$, and $R_0 = \sqrt{4.0004}$, and (2.6) tells us that

$$\|A_{k,\eta}^{-1}\| \leq B,$$

where B is as defined in §2.2. However, we see from Table 4.11 that this bound is a gross overestimate, at least provided we choose η carefully. For the definition of B implies that, whatever the choice of $\eta \in \mathbb{R} \setminus \{0\}$,

$$B > \frac{1}{2} + \left[\left(\frac{\delta_+}{\delta_-} + \frac{4\delta^{*2}}{\delta_-^2}\right)\left(\frac{\delta_+}{\delta_-} + \frac{\delta^{*2}}{\delta_-^2}\right)\right]^{1/2} > 2\frac{\delta^{*2}}{\delta_-^2} = 2 \times 10^4$$

for this geometry. If we choose $\eta = k$ for small k then, indeed, we see significant blowup as $k \to 0$, as for the case of the square (indeed the values of $\|A_{k,\eta}^{-1}\|$ are similar). But, if we choose $\eta = \eta^* := 1/R_0(1 - \ln(kR_0))$, we know from Theorem 2.11 that $\|A_{k,\eta}^{-1}\|$ must stay bounded as $k \to 0$. In fact we see some mild, logarithmic growth in Table 4.11, but $\|A_{k,\eta^*}^{-1}\|$ is never larger than 26 for the range of k shown.

For the computations in Table 4.11 we used 100 elements on each boundary segment. Comparing the algebraic rates p associated with $\|A_{k,k}^{-1}\|$ for the first three wavenumbers $k = 10^{-5}, 10^{-4}, 10^{-3}$ it appears possible that the discretisation does not fully resolve $\|A_{k,k}^{-1}\|$ for $k = 10^{-5}$ and that the exact value may be higher. However, due to convergence issues of the underlying singular value decomposition for the norm computation no finer discretisation could be used here.

4.7. Rectangular cavity. In the last two numerical examples we explore trapping domains, as studied theoretically in §2.5. The rectangular cavity in Figure 4.1 is defined by the polygon with the following coordinates: $p_0 = 0$, $p_1 = (-c, 0)$, $p_2 = (-c, -\ell)$, $p_3 = (\ell, -\ell)$, $p_4 = (\ell, 2c - \ell)$, $p_5 = (-c, 2c - \ell)$, $p_6 = (-c, 2a)$, $p_7 = (0, 2a)$. Here, $a = \pi/10$, $c = 1$, and $\ell = c - a$. The width of the cavity is $2a = \pi/5$. Hence we expect resonance values in the negative half of the complex plane close to $k = 5m$, $n \in \mathbb{N}$ (see [6, Figure 5.12] for numerical computations of exterior resonances for this cavity). Since for $k = 5m$ the width of the cavity is an integer multiple of half a wavelength, Theorem 2.7 applies and implies that, for $k = 5m$ and

k	$\|A_{k,k}\|$	$\|A_{k,k}^{-1}\|$	p	$\|A_{k,\eta^*}\|$	$\|A_{k,\eta^*}^{-1}\|$	p
10^{-5}	1.978	3087.76		1.978	25.165	
10^{-4}	1.978	924.25	-0.53	1.978	21.533	-0.07
10^{-3}	1.978	128.19	-0.86	1.978	17.581	-0.09
10^{-2}	1.978	45.28	-0.45	1.978	14.078	-0.10
10^{-1}	1.978	14.43	-0.50	1.978	10.384	-0.13
1	2.050	4.53	-0.50	3.310	3.570	-0.46

TABLE 4.11

Rectangle of side lengths 2 and 0.02. *Galerkin BEM approximations to* $\|A_{k,k}\|$, $\|A_{k,k}^{-1}\|$, $\|A_{k,\eta^*}\|$ *, and* $\|A_{k,\eta^*}^{-1}\|$.

$m \in \mathbb{N}$,

$$\|A_{k,\eta}^{-1}\| \geq Ck^{9/10},$$

for both $\eta = k$ and $\eta = k^{2/3}$. Hence, as $k \to \infty$, $\|A_{k,k}^{-1}\|$ will grow, a behaviour not observed in the previous examples.

Estimates for $\|A_{k,k}\|$, $\|A_{k,k}^{-1}\|$, $\|A_{k,k^{2/3}}\|$ and $\|A_{k,k^{2/3}}^{-1}\|$ for various k are shown in Table 4.12 below. As expected, the value of $\|A_{k,k}^{-1}\|$ grows at a rate at least as fast as $k^{9/10}$, and cond $A_{k,k}$ grows at approximately the rate $k^{7/5}$ predicted by Theorem 2.12. The growth of $\|A_{k,k^{2/3}}^{-1}\|$ and cond $A_{k,k^{2/3}}$ are more erratic. Theorem 2.5 implies that $\|D_k\| \geq Ck^{1/4}$, and $\|S_k\| \leq Ck^{1/2}$ by (2.10), so that, for this obstacle, $\|A_{k,k^{2/3}}\| \geq Ck^{1/4}$. Thus the theoretical lower bound for cond $A_{k,k^{2/3}}$ is cond $A_{k,k^{2/3}} \geq Ck^{23/20}$, a slower rate of growth than that proved for cond $A_{k,k}$. Nevertheless, cond $A_{k,k} <$ cond $A_{k,k^{2/3}}$ for the larger values of k in Table 4.12.

k	$\|A_{k,k}\|$	p	$\|A_{k,k}^{-1}\|$	p	$\|A_{k,k^{2/3}}\|$	p	$\|A_{k,k^{2/3}}^{-1}\|$	p
5	4.835		1.969		3.575		3.075	
10	5.201	0.11	3.121	0.66	3.580	0.00	5.990	0.96
20	5.629	0.11	5.539	0.83	3.594	0.01	9.348	0.64
40	6.182	0.14	10.322	0.90	3.790	0.08	19.029	1.03
80	8.112	0.39	19.774	0.94	4.223	0.16	28.528	0.58
160	11.066	0.45	38.351	0.96	4.788	0.18	173.563	2.60
320	15.254	0.46	75.156	0.97	5.483	0.20	277.480	0.68

TABLE 4.12

Rectangular cavity. *Galerkin BEM approximations to* $\|A_{k,k}\|$, $\|A_{k,k}^{-1}\|$, $\|A_{k,k^{2/3}}\|$ *and* $\|A_{k,k^{2/3}}^{-1}\|$.

4.8. Elliptic cavity. The elliptic cavity in Figure 4.1 is defined by two elliptic arcs. The first one is parameterised as $(\cos t, 0.5 \sin t)$, $t \in [-\phi_0, \phi_0]$, with $\phi_0 = 7\pi/10$ and the second arc is defined by $(1.3 \cos t, 0.6 \sin t)$, $t \in [-\phi_1, \phi_1]$, with $\phi_1 = \arccos(\frac{1}{1.3} \cos \phi_0)$. As discussed in §2.5, we expect large values of $\|A_{k,k}^{-1}\|$ at k values corresponding to so-called 'bouncing ball' eigenmodes of the inner ellipse, which has semi-axes 1 and 0.5. Some of these modes, discussed in detail in the appendix, are shown in Figure 4.3. As k grows, these modes become more localized around the centre of the ellipse, i.e. around the stable periodic orbit (see §2.5 and the appendix).
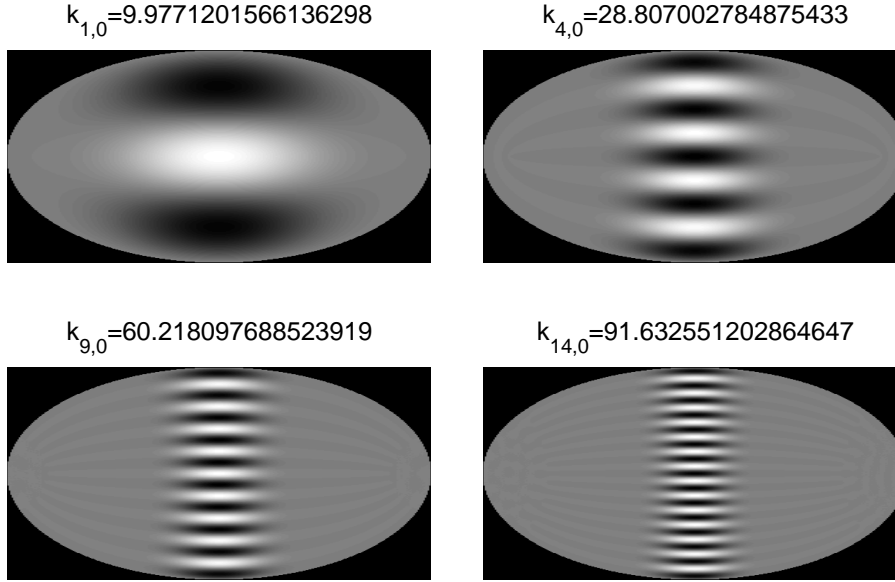
$k_{1,0}=9.9771201566136298$ $k_{4,0}=28.807002784875433$

$k_{9,0}=60.218097688523919$ $k_{14,0}=91.632551202864647$

FIG. 4.3. *Some exponentially localised modes of the ellipse associated with zeros of the radial Mathieu function of order* 0*. In the notation of the appendix, the modes plotted are* $u_{m,0}$ *for* $m = 1, 4, 9,$ *and* 14*, corresponding to the wavenumbers* $k_{m,0}$*,* $m = 1, 4, 9, 14$*.*

Estimates for $\|A_{k,k}\|$ and $\|A_{k,k}^{-1}\|$ for the four wavenumbers from Figure 4.3 are shown in Table 4.13. We expect, from Theorems 2.8 and 2.13, exponential growth of $\|A_{k,k}^{-1}\|$ and cond $A_{k,k}$ with k. Comparing the values of $\|A_{k,k}^{-1}\|$ for the two lowest wavenumbers a large growth is clearly visible. However, the growth of $\|A_{k,k}^{-1}\|$ then levels off. It may be that the given discretisation with about 10 elements per wavelength is not sufficient to resolve the large norm of the inverse, or that, due to discretisation error, the resonance wavenumber k is shifted somewhat from the theoretically predicted value. Repeating the computation with approximately 20 elements per wavelength, we see the computed values for $\|A_{k,k}^{-1}\|$ for larger k are significantly larger now. However, the growth of the inverse still levels off, and we do not observe exponential growth even with this finer discretisation. We note, however, that with this finer discretisation we see, at the highest value of k, a condition number cond $A_{k,k} \approx 140,000$, hugely larger than the values observed in any of the previous examples, including the rectangular cavity.

k	$\|A_{k,k}\|$	p	$\|A_{k,k}^{-1}\|$	$\|A_{k,k}^{-1}\|$ (refined)
9.977	5.595		67.3	70.1
28.807	7.294	0.25	2829.9	9182.7
60.218	8.820	0.26	5265.0	13373.8
91.633	10.144	0.33	6543.8	14258.6

TABLE 4.13

Elliptic cavity. *Galerkin BEM approximations to* $\|A_{k,k}\|$ *and* $\|A_{k,k}^{-1}\|$*. For* $\|A_{k,k}^{-1}\|$ *the results of a refined computation with twice the number of degrees of freedom and approximately* 20 *elements per wavelength are shown.*

5. Conclusions. In this paper we have, in §2, summarised what is known regarding upper and lower bounds on the norms of the acoustic single- and double-layer potential operators, S_k and D_k, and the combined layer potential operator $A_{k,\eta}$, with an emphasis on how these bounds behave as a function of frequency, and the influence of the shape of the boundary. We have also proved sharper upper bounds on $\|S_k\|$ and $\|A_{k,\eta}\|$ for low k, have summarised what upper and lower bounds on $\|A_{k,\eta}^{-1}\|$ are known, and have shown that exponential growth of $\|A_{k,\eta}^{-1}\|$ is possible as $k \to \infty$ through some sequence of wave numbers, in the case of a certain class of 2D trapping obstacles. Finally, we have discussed the condition number cond $A_{k,\eta}$, proving that it remains bounded as $k \to 0$ with appropriate choices of the coupling parameter η, and showing that, while it increases as $k \to \infty$ only as fast as $k^{1/3}$ for a circle or sphere, and at the rate $k^{1/2}$ for a starlike polygon, it grows exponentially, as k increases through some sequence, for certain trapping obstacles.

In §3 we have explored the implications of these results for Galerkin BEM discretisations of these operators, showing that the norms of the Galerkin BEM matrices converge to the norms of the operators that they discretise, as the mesh is refined, and provided an orthonormal basis is used. Convergence to $\|A_{k,\eta}^{-1}\|$ of the norm of the inverse of the matrix corresponding to $A_{k,\eta}$ has also been proved in the case that Γ is C^1. Thus we expect that the norm bounds at the continuous level in §2 will apply also at the discrete level if the mesh is sufficiently refined.

This has been confirmed in §4 where we have explored a range of numerical examples, including shapes that are convex (both smooth and non-smooth), non-convex but starlike, and non-starlike trapping obstacles. The quantitative upper and lower bounds stated in §2 are found to be upper and lower bounds also at the discrete level, and to be rather sharp in many of the examples. In almost all cases the observed rate of growth of norms and condition numbers as k increases is in accordance with the possible range of behaviour suggested by the upper and lower bounds from §2, with the rates of growth mainly closer to the lower bounds of §2.4. The exception is that the exponential growth predicted in Theorems 2.8 and 2.13 is not observed numerically in the 'Elliptic cavity' example, at least at the discretisations we use. On the other hand, the condition numbers observed in this case are as high as 140,000 and the values of $\|A_{k,k}^{-1}\|$ as high as 14,000, which contrasts with $\|A_{k,k}^{-1}\| \approx 1$ in all the cases where the scatterer Ω is starlike.

REFERENCES

[1] M. Abramowitz and I. Stegun, Handbook of Mathematical Functions, Dover, New York, 1972.
[2] S. Agmon, Lectures on Exponential Decay of Solutions of Second-Order Elliptic Equations, Princeton University Press, Princeton NJ, 1982.
[3] S. Amini, On the choice of the coupling parameter in boundary integral equation formulations of the exterior acoustic problem, Appl. Anal., **35**, (1990), 75–92.
[4] S. Amini, Boundary integral solution of the exterior acoustic problem, Comput. Mech., **13**, (1993), 2–11.
[5] L. Banjai and S. Sauter, A refined Galerkin error and stability analysis for highly indefinite variational problems, SIAM J. Numer. Anal. **45**, (2007), 37–53.
[6] T. Betcke and E.A. Spence, Numerical estimation of coercivity constants for boundary integral operators in acoustic scattering, submitted to SIAM J. Numer. Anal.
[7] O. P. Bruno and A. L. Kunyansky, Surface scattering in three dimensions: an accelerated high-order solver, Proc. R. Soc. Lond. A **457**, (2001), 2921–2934.
[8] O. P. Bruno, Private communication, 2007.
[9] S. N. Chandler-Wilde and S. Langdon, A Galerkin boundary element method for high frequency scattering by convex polygons, SIAM J. Numer. Anal. **45**, (2007), 610–640.
[10] S. N. Chandler-Wilde, I. G. Graham, S. Langdon and M. Lindner, Condition number estimates

for combined potential boundary integral operators in acoustic scattering, J. Int. Eqn. Appl. **21**, (2009), 229–279.

[11] S. N. Chandler-Wilde and P. Monk, Wave-number-explicit bounds in time-harmonic scattering, SIAM J. Math. Anal. **39**, (2008), 1428–145.

[12] D. L. Colton and R. Kress, Integral equation methods in scattering theory, John Wiley, New York, 1983.

[13] ——, Inverse Acoustic and Electromagnetic Scattering Theory, Springer Verlag, 2nd Ed., 1992.

[14] Digital Library of Mathematical Functions, Release date 2010-05-07, National Institute of Standards and Technology from `http://dlmf.nist.gov/`.

[15] V. Dominguez, I. G. Graham, and V. P. Smyshlyaev, A hybrid numerical-asymptotic boundary integral method for high-frequency acoustic scattering, Numer. Math. **106**, (2007) 471–510.

[16] E. B. Fabes, M. Jodeit, and N.M. Riviere, Potential techniques for boundary value problems on C^1 domains, Acta Math., **141**, (1978) 165–186.

[17] K. Giebermann, Schnelle Summationsverfahren zur numerischen Lösung von Integralgleichungen für Streuprobleme im $\mathbb{R}^3$, PhD Thesis, Universität Karlsruhe, Germany, 1997.

[18] P. D. Hislop and I. M. Segal, Introduction to spectral theory: with applications to Schrödinger operators, Springer, New York, 1995.

[19] J. B. Keller, Semiclassical mechanics, SIAM Rev., **27**, (1985), 485–504.

[20] R. Kress, Minimizing the condition number of boundary integral-operators in acoustic and electromagnetic scattering, Q. J. Mech. Appl. Math., **38**, (1985), 323–341.

[21] R. Kress and W. T. Spassov, On the condition number of boundary integral operators for the exterior Dirichlet problem for the Helmholtz equation, Numer. Math., **42**, (1983), 77–95.

[22] R. Kress, Linear Integral Equations, Springer, New York, 2nd Edition, 1999.

[23] V. F. Lazutkin, "Semiclassical asymptotics of eigenfunctions", in Encyclopedia of Mathematical Sciences, Volume 34, Partial Differential Equations V, M. V. Fedoryuk (Editor), Springer, New York, 1999, p. 133.

[24] M. Löhndorf and J. M. Melenk, Wavenumber-explicit hp-BEM for high frequency scattering, ASC Report 2/2010, Institute for Analysis and Scientific Computing, Vienna University of Technology - TU Wien, 2010

[25] N. W. McLachlan, Theory and Application of Mathieu Functions, Oxford University Press, Oxford, 1947.

[26] W. McLean, Strongly Elliptic Systems and Boundary Integral Equations, Cambridge University Press, Cambrideg, 2000.

[27] J.M. Melenk, Mapping properties of combined field Helmholtz boundary integral operators, ASC Report 1/2010, Institute for Analysis and Scientific Computing, Vienna University of Technology - TU Wien, 2010.

[28] S. Prössdorf and B. Silbermann, Numerical Analysis for Integral and Related Operator Equations, Birkhäuser, 1991.

[29] A. G. M. Neves, Eigenmodes and eigenfrequencies of vibrating elliptic membranes: a Klein oscillation theorem and numerical calculations, Comm. Pure Appl. Anal., **9**, (2010), 611–624.

[30] J. Toth, Eigenfunction decay estimates in the quantum integrable case, Duke Math. J., **93**, (1998), 231–255.

[31] G. Verchota, Layer potentials and regularity for the Dirichlet problem for Laplace's equation in Lipschitz domains, J. Funct. Anal., **59**, (1984), 572–611.

[32] K.F. Warnick and W.C. Chew, Error analysis of the moment method, IEEE Ant. Prop. Mag. **46**, (2004), 38–53.

[33] K.F. Warnick and W.C. Chew, On the spectrum of the electric field integral equation and the convergence of the moment method, Int. J. Numer. Meth. Engng. **51**, (2001), 31–56.

[34] K.F. Warnick and W.C. Chew, Convergence of moment-method solutions of the electric field integral equation for a 2-D open cavity, Microwave Optical Tech. Letters **23**, (1999), 212–218.

[35] H. B. Wilson and R.W. Scharstein, Computing elliptic membrane high frequencies by Mathieu and Galerkin methods, J. Eng. Math., **57**, (2007), 41–55.

Appendix: Eigenmodes of the Ellipse. In this appendix we summarise key properties of eigenmodes of the Laplacian in an elliptical domain. Suppose $a_1 > a_2 > 0$ and let $E = \{(x_1, x_2) \in \mathbb{R}^2 : (x_1/a_1)^2 + (x_2/a_2)^2 \leq 1\}$ be the ellipse with semi-major axis a_1 and semi-minor axis a_2. Then we study in this appendix certain Laplace

eigenmodes $u \in C^2(\bar{E})$ satisfying

$$\Delta u + k^2 u = 0 \text{ in } E, \quad u = 0 \text{ on } \partial E, \tag{A.1}$$

for some $k > 0$.

Let $a = \sqrt{a_1^2 - a_2^2} = a_1 \varepsilon$, where $\varepsilon = \sqrt{1 - a_2^2/a_1^2}$ is the eccentricity of the ellipse, and introduce elliptical coordinates (μ, ν), defined by

$$x_1 = a \cosh \mu \cos \nu \quad \text{and} \quad x_2 = a \sinh \mu \sin \nu,$$

in terms of which

$$E = \{(a \cosh \mu \cos \nu, a \sinh \mu \sin \nu) : 0 \le \mu \le \mu_0, \ 0 \le \nu < 2\pi\},$$

where $\mu_0 := \tanh^{-1}(a_2/a_1)$. It is well known (see e.g. [35]) that the Laplace operator separates in elliptical coordinates, and that in this coordinate system the Helmholtz equation can be written as

$$\left(\frac{\partial^2}{\partial \mu^2} + \frac{\partial^2}{\partial \nu^2} + k^2 a^2 (\sinh^2 \mu + \sin^2 \nu) \right) u = 0. \tag{A.2}$$

Seeking separation of variables solutions in the form $u(x) = M(\mu)N(\nu)$, we see that (A.2) implies that N satisfies the circumferential (or standard) Mathieu equation

$$N''(\nu) + (\alpha - 2q \cos 2\nu)N(\nu) = 0, \tag{A.3}$$

while M satisfies the radial (or modified) Mathieu equation

$$M''(\mu) - (\alpha - 2q \cosh 2\mu)M(\mu) = 0. \tag{A.4}$$

In these equations

$$q = \frac{1}{4}(ka)^2 = \frac{1}{4}(ka_1)^2(1 - (a_2/a_1)^2)$$

and α is a separation constant. The solutions to (A.3) that we are interested in are the solutions of period 2π, satisfying $N(0) = N(2\pi)$ and $N'(0) = N'(2\pi)$. Since $N(-\nu)$ is such a solution if $N(\nu)$ is, it is clear that we may restrict attention to periodic solutions of (A.3) that are either even or odd.

For this paper it is enough to focus on the even periodic solutions, so that we seek solutions N of (A.3) which satisfy $N'(0) = N'(\pi)$. This is an eigenvalue problem in which the eigenvalue is the separation constant α. Standard Sturm-Liouville theory tells us that, for each value of the parameter $q > 0$, there are a countable number of eigenvalues $\alpha = a_n(q)$, $n = 0, 1, \ldots$, with $a_0(q) < a_1(q) < \ldots$ and $a_n(q) \to \infty$ as $n \to \infty$ (we use in this appendix the standard notation for these eigenvalues and the corresponding eigenfunctions, see e.g. [14, §28.2(v)]). Further, to the eigenvalue $a_n(q)$ there corresponds a unique (to within multiplication by a constant), real-valued eigenfunction $N(\nu)$, which is usually denoted by $\mathrm{ce}_n(\nu, q)$ (for the standard normalization of ce_n see [14, §28.2(vi)]). The standard Sturm-Liouville theory tells us that $\mathrm{ce}_n(\nu, q)$ has precisely n zeros in $(0, \pi)$. It is easy to see that $\mathrm{ce}_n(\nu, q) \pm \mathrm{ce}_n(\pi - \nu, q)$ is also an eigenfunction corresponding to $\alpha = a_n(q)$; thus the uniqueness of the normalised eigenfunction implies that, for $\nu \in \mathbb{R}$ and $n \ge 0$,

$$\mathrm{ce}_n(\nu, q) = \mathrm{ce}_n(\pi - \nu, q) \text{ if } n \text{ is even}, \quad \mathrm{ce}_n(\nu, q) = -\mathrm{ce}_n(\pi - \nu, q) \text{ if } n \text{ is odd}. \tag{A.5}$$

Given that $\alpha = a_n(q)$, for some $n \geq 0$, and that $N = \mathrm{ce}_n(\cdot, q)$, it is a standard result (e.g. [25]) that $u(x) = M(\mu)N(\nu)$ satisfies the Helmholtz equation (A.1) in E if and only if $M \in C^2(\mathbb{R})$ is an even function that satisfies (A.4). This uniquely specifies M to within multiplication by a constant. The standard notation for this (real-valued) solution is $M(\mu) = \mathrm{Mc}_n^{(1)}(\mu, q)$; see [14, §28.20(iv)] for the standard normalization. Thus we see that $u(x) = M(\mu)N(\nu) = \mathrm{Mc}_n^{(1)}(\mu, q)\mathrm{ce}_n(\nu, q)$ satisfies the full eigenvalue problem (A.1) if and only if

$$\mathrm{Mc}_n^{(1)}(\mu_0, q) = 0. \tag{A.6}$$

The complication in computing eigenmodes of the ellipse (for methods see [35, 29]) is that it is a multi-parameter spectral problem: to satisfy (A.6) we have to find a pair (α, q) such that, simultaneously, (A.3) has a periodic solution and (A.4) has a solution which is even if N is even and which vanishes at μ_0. Neves [29] gives a proof based on multi-parameter spectral theory that for each pair $(m, n) \in \{0, 1, \ldots\}^2$ there exists a unique $q_{m,n} > 0$ such that (A.6) holds with $\mathrm{Mc}_n^{(1)}(\cdot, q_{m,n})$ having m zeros in $(0, \mu_0)$. The function

$$u(x) = u_{m,n}(x) := \mathrm{Mc}_n^{(1)}(\mu, q_{m,n})\mathrm{ce}_n(\nu, q_{m,n}) \tag{A.7}$$

is then an eigenfunction of (A.1) for $k = k_{m,n} := \sqrt{4q_{m,n}}/a$. It is well known (e.g. [12]) that the eigenvalues of the Laplace operator have infinity as the only accumulation point, so that $k_{m,n} \to \infty$ as $m + n \to \infty$.

For some $\nu_0 \in (0, \pi/2)$ let

$$E_{\nu_0} := \{(a \cosh \mu \cos \nu, a \sinh \mu \sin \nu) : 0 \leq \mu < \mu_0, \ |\nu| < \nu_0 \text{ or } |\pi - \nu| < \nu_0\}$$
$$\supset \{(x_1, x_2) \in E : |x_1| > a_1 \cos \nu_0\}.$$

Let

$$\rho_{\nu_0}(m, n) := \left\{ \frac{\int_{E_\nu}(u_{m,n})^2 \, dx}{\int_E (u_{m,n})^2 \, dx} \right\}^{1/2}.$$

Our particular interest in this appendix is in families of eigenfunctions that are exponentially localised around the periodic orbit $\{(0, x_2) : |x_2| \leq a_2\}$. In particular we will show below that the family $u_{m,0}$, $m = 0, 1, \ldots$ is so localised; precisely, we will show that, for all $\nu_0 \in (0, \pi/2)$, there exists $\beta > 0$ such that $\rho_{\nu_0}(m, 0) = O(\mathrm{e}^{-\beta k_m})$ as $m \to \infty$.

Noting (A.5), we see that

$$\int_{E_\nu}(u_{m,n})^2 \, dx = 4a^2 \int_0^{\nu_0} \int_0^{\mu_0} (\sinh^2 \mu + \sin^2 \nu) \left(\mathrm{Mc}_n^{(1)}(\mu, q_{m,n})\mathrm{ce}_n(\nu, q_{m,n}) \right)^2 d\mu d\nu.$$

Thus, defining

$$M_j := \int_0^{\mu_0} (\sinh \mu)^{2j} \left(\mathrm{Mc}_n^{(1)}(\mu, q_{m,n}) \right)^2 d\mu, \quad I_s(m, n) := \int_0^s (\mathrm{ce}_n(\nu, q_{m,n}))^2 \, d\nu,$$

it holds that

$$(\rho_{\nu_0}(m, n))^2 \leq \frac{(M_1 + M_0 \sin^2 \nu_0) I_{\nu_0}(m, n)}{M_1 I_{\pi/2}(m, n) + M_0 \sin^2 \nu_0 (I_{\pi/2}(m, n) - I_{\nu_0}(m, n))}$$
$$\leq \frac{I_{\nu_0}(m, n)}{I_{\pi/2}(m, n) - I_{\nu_0}(m, n)}. \tag{A.8}$$

33

It is sufficient for the needs of this paper to estimate the asymptotics as $m \to \infty$ of $\rho_{\nu_0}(m, n)$ for $n = 0$, and so we will restrict our attention to this case. For this purpose, and abbreviating $q_{m,0}$ as q_m and $k_{m,0}$ as k_m, recall that $\mathrm{ce}_0(\nu, q_m)$ satisfies (A.3) with $q = q_m$ and with $\alpha = a_0(q_m)$. Now the asymptotics of the eigenvalue $a_0(q)$ as $q \to \infty$ are known. From [14] we have that

$$a_0(q) = -2q + q^{1/2} + O(1) \tag{A.9}$$

as $q \to \infty$. Thus we see that, for m large and with $N = \mathrm{ce}_0(\cdot, q_m)$, the coefficient $a_0(q_m) - 2q_m \cos 2\nu$ of $N(\nu)$ in (A.3) is negative except in small neighbourhoods of $\pm\pi/2$ of length $O(q_m^{-1/4}) = O(k_m^{-1/2})$. It is this which causes the exponential localisation of $u_{m,0}$ around the periodic orbit.

To see this localization completely explicitly, we will use the following lemma which depends on standard weighted space arguments (cf. [2], [18, §3]). In this lemma and subsequently $BC(\mathbb{R})$ denotes the set of functions $\phi : \mathbb{R} \to \mathbb{R}$ that are bounded and continuous and $BC^k(\mathbb{R}) := \{\phi \in BC(\mathbb{R}) : \phi^{(j)} \in BC(\mathbb{R}) \text{ for } j = 0, 1, \ldots, k\}$. As usual, $H^s(\mathbb{R})$, for $s \geq 0$, denotes the standard Sobolev space of order s (which in this appendix we take to be a space of real-valued functions). For $\beta > 0$ and $\alpha \geq 0$ let $w_{\beta,\alpha} : \mathbb{R} \to \mathbb{R}$ denote the weight function

$$w_{\beta,\alpha}(s) = \exp\left(-\beta\sqrt{\alpha^2 + s^2}\right),$$

and, for $\phi \in BC(\mathbb{R})$, let

$$\|\phi\|_{\beta,\alpha} := \left\{\int_{-\infty}^{\infty} (w_{\beta,\alpha}(s)\phi(s))^2 ds\right\}^{1/2} < \infty.$$

LEMMA A.1. *Suppose that $p \in BC(\mathbb{R})$ and that, for some $c > 0$, $p(s) \leq -c^2 < 0$, $s \in \mathbb{R}$. Suppose also that $g \in BC(\mathbb{R})$, $v \in BC^2(\mathbb{R})$, and*

$$v''(s) + p(s)v(s) = g(s), \quad s \in \mathbb{R}.$$

Then, for $0 < \beta < c$ and $\alpha \geq 0$,

$$\|v\|_{\beta,\alpha} \leq \frac{1}{c^2 - \beta^2} \|g\|_{\beta,\alpha}. \tag{A.10}$$

Proof. Suppose $\beta > 0$ and $\alpha > 0$. Define $\psi \in BC^2(\mathbb{R}) \cap H^2(\mathbb{R})$ by $\psi(s) = w_{\beta,a}(s)v(s)$, $s \in \mathbb{R}$. Then it is an easy calculation, abbreviating $w_{\beta,\alpha}$ as w, that

$$\psi'' - 2\frac{w'}{w}\psi' + \left(p + 2\left(\frac{w'}{w}\right)^2 - \frac{w''}{w}\right)\psi = wg.$$

Multiplying by a test function ϕ and integrating by parts, we see that

$$a(\psi, \phi) = b(\phi), \quad \phi \in H^1(\mathbb{R}), \tag{A.11}$$

where the bilinear form $a : H^1(\mathbb{R}) \times H^1(\mathbb{R}) \to \mathbb{R}$ and the bounded linear functional $b : H^1(\mathbb{R}) \to \mathbb{R}$ are defined by

$$a(\phi, \psi) := \int_{-\infty}^{\infty} \left(\psi'\phi' + 2\frac{w'}{w}\psi'\phi - \left(p + 2\left(\frac{w'}{w}\right)^2 - \frac{w''}{w}\right)\psi\phi\right) ds,$$

$$b(\phi) := -\int_{-\infty}^{\infty} wg\phi \, ds.$$

34

Since $w'/w, w''/w \in BC(\mathbb{R})$, the bilinear form a is bounded. For $\phi \in H^1(\mathbb{R})$,

$$a(\phi, \phi) = \int_{-\infty}^{\infty} \left((\phi')^2 + \frac{w'}{w}(\phi^2)' - \left(p + 2\left(\frac{w'}{w}\right)^2 - \frac{w''}{w} \right) \phi^2 \right) ds$$

$$= \int_{-\infty}^{\infty} \left((\phi')^2 - \left(p + \left(\frac{w'}{w}\right)^2 \right) \phi^2 \right) ds,$$

where the last step follows by integration by parts, on noting that $(w'/w)' = w''/w - (w'/w)^2$. Since $-p - (w'/w)^2 \geq c^2 - \beta^2$, a is coercive if $\beta < c$, with

$$a(\phi, \phi) \geq \|\phi\|_1^2, \text{ where } \|\phi\|_1 := \left(\int_{-\infty}^{\infty} \left((\phi')^2 + \left(c^2 - \beta^2 \right) \phi^2 \right) ds \right)^{1/2}.$$

Applying the Lax-Milgram lemma, it follows from (A.11) that

$$\sqrt{c^2 - \beta^2}\|v\|_{\beta,\alpha} \leq \|\psi\|_1 \leq \|b\| \leq \frac{\|g\|_{\beta,\alpha}}{\sqrt{c^2 - \beta^2}},$$

where $\|b\|$ denotes the norm of the linear functional $b : H^1(\mathbb{R}) \to \mathbb{R}$, with $H^1(\mathbb{R})$ given the norm $\|\cdot\|_1$. Hence (A.10) holds for $\beta > 0$ and $\alpha > 0$, and so also for $\alpha = 0$ by the dominated convergence theorem. $\square$

To apply this lemma to (A.3), let $v := \mathrm{ce}_0(\cdot, q)$ and define $p \in BC(\mathbb{R})$ by $p(\nu) = a_0(q) - 2q\cos 2\nu$, $\nu \in \mathbb{R}$. For $c > 0$ write p as $p = p_c^- + p_c^+$ where $p_c^- := \min(-c^2, p)$ and $p_c^+ := p - p_c^-$, and set $g_c := -p_c^+ v$. Then $v'' + p_c^- v = g_c$, and applying Lemma A.1 with $\alpha = 0$ it follows that, for $\nu_0 \in (0, \pi/2)$,

$$\left\{ 2 \int_0^{\nu_0} v^2 ds \right\}^{1/2} \leq \mathrm{e}^{\beta\nu_0}\|v\|_{\beta,0} \leq \frac{\mathrm{e}^{\beta\nu_0}}{c^2 - \beta^2} \|g_c\|_{\beta,0},$$

for $0 < \beta < c$. For $-2q < a_0(q) + c^2 < 2q$ we see that $g_c(\nu) = 0$ if $|\nu - j\pi| \leq \nu_c$, for some $j \in \mathbb{Z}$, where $\nu_c \in (0, \pi/2)$ is given by

$$\nu_c := \frac{1}{2} \cos^{-1}\left(\frac{a_0(q) + c^2}{2q} \right). \tag{A.12}$$

Thus, and since $0 \leq p_c^+ \leq a_0(q) + 2q + c^2 < 4q$, it follows that

$$\|g_c\|_{\beta,0}^2 = 2 \int_0^{\infty} \mathrm{e}^{-2\beta s}(g_c(s))^2 ds$$

$$\leq 8q \sum_{j=0}^{\infty} \int_{j\pi+\nu_c}^{(j+1)\pi-\nu_c} \mathrm{e}^{-2\beta s}(v(s))^2 ds$$

$$\leq 8q \frac{\mathrm{e}^{-2\beta\nu_c}}{1 - \mathrm{e}^{-2\beta\pi}} \int_0^{\pi} v^2 ds.$$

So

$$\left\{ \int_0^{\nu_0} v^2 ds \right\}^{1/2} \leq 2\sqrt{2q} \frac{\mathrm{e}^{-\beta(\nu_c-\nu_0)}}{(c^2 - \beta^2)(1 - \mathrm{e}^{-2\beta\pi})^{1/2}} \left\{ \int_0^{\pi/2} v^2 ds \right\}^{1/2}$$

and choosing $\beta = c^2(\nu_c - \nu_0)/(1 + \sqrt{1 + (\nu_c - \nu_0)^2 c^2}) \in (0, c)$, which minimises $\mathrm{e}^{-\beta(\nu_c - \nu_0)}/(c^2 - \beta^2)$, we find that

$$\left\{\int_0^{\nu_0} v^2 ds\right\}^{1/2} \le \frac{(\nu_c - \nu_0)^2 \sqrt{2q}\,\mathrm{e}^{-\gamma}}{\gamma\,(1 - \mathrm{e}^{-4\gamma\pi})^{1/2}} \left\{\int_0^{\pi/2} v^2 ds\right\}^{1/2}, \tag{A.13}$$

where $\gamma := \delta/(1 + \sqrt{1 + \delta})$, with $\delta := c^2(\nu_c - \nu_0)^2$, provided that $-2q < a_0(q) + c^2 < 2q$ and $0 < \nu_0 < \nu_c$. Thus, assuming that $-a_0(q)/(2q) \in (-1, 0)$ (which is certainly the case for all sufficiently large q by (A.9)), and provided

$$0 < \nu_0 < \frac{1}{2}\cos^{-1}\left(\frac{a_0(q)}{2q}\right), \tag{A.14}$$

(A.13) holds for $0 < c < \sqrt{2q\cos 2\nu_0 - a_0(q)}$. It particular, choosing

$$c := \frac{1}{2}\sqrt{2q\cos 2\nu_0 - a_0(q)}, \tag{A.15}$$

we obtain the following result in which the formula for δ follows from $\delta = c^2(\nu_c - \nu_0)^2$, with c given by (A.15) and ν_c by (A.12), recalling that $\cos^{-1}(-1 + \alpha) = \pi - 2\sin^{-1}\sqrt{\alpha/2}$, for $0 \le \alpha \le 2$.

THEOREM A.2. *Let $v := \mathrm{ce}_0(\cdot, q)$ and suppose that $-a_0(q)/(2q) \in (-1, 0)$ (which certainly holds for all sufficiently large q). Then, provided ν_0 satisfies (A.14), it holds that*

$$\left\{\int_0^{\nu_0} v^2 ds\right\}^{1/2} \le \frac{\phi_0^2 \sqrt{2q}\,\mathrm{e}^{-\gamma}}{\gamma\,(1 - \mathrm{e}^{-4\gamma\pi})^{1/2}} \left\{\int_0^{\pi/2} v^2 ds\right\}^{1/2},$$

where $\phi_0 = \pi/2 - \nu_0$, $\gamma = \delta/(1 + \sqrt{1 + \delta})$,

$$\delta = q(\sin^2 \phi_0 - r(q))\left(\phi_0 - \sin^{-1}\left(\frac{1}{2}\sqrt{\sin^2 \phi_0 + 3r(q)}\right)\right)^2.$$

and $r(q) := (1 + a_0(q)/(2q))/2$.

By (A.9), $r(q) \sim q^{-1/2}/2$ as $q \to \infty$. Thus, in the above theorem, as $q \to \infty$ δ has the asymptotic behaviour $\delta \sim q\sin^2 \phi_0 \left(\phi_0 - \sin^{-1}\left(\frac{1}{2}\sin \phi_0\right)\right)^2$. Thus, and since $\sin^{-1}\left(\frac{1}{2}\sin \phi_0\right) < \frac{1}{2}\phi_0$, it holds that $\delta > \frac{1}{4}q\phi_0^2 \sin^2 \phi_0$ for all sufficiently large q. Further, $\gamma = \delta^{1/2} - 1 + O(\delta^{-1/2})$ as $\delta \to \infty$. Thus the above theorem has the following corollary.

COROLLARY A.3. *Let $v := \mathrm{ce}_0(\cdot, q)$. Then, for every $\nu_0 \in (0, \pi/2)$, it holds for all sufficiently large q that*

$$\left\{\int_0^{\nu_0} v^2 ds\right\}^{1/2} \le \frac{2\sqrt{2}\,\mathrm{e}\,\phi_0}{\sin \phi_0}\exp\left(-\frac{1}{2}\sqrt{q}\phi_0 \sin \phi_0\right)\left\{\int_0^{\pi/2} v^2 ds\right\}^{1/2},$$

where $\phi_0 = \pi/2 - \nu_0$.

Applying this corollary with $q = q_m = \frac{1}{4}(k_m a)^2$, and recalling the bound (A.8), and that $a = a_1 \varepsilon$, where ε is the eccentricity of the ellipse, and that $\phi_0/\sin \phi_0 < \pi/2$, we see that, for every $\nu_0 \in (0, \pi/2)$, it holds for all sufficiently large m that

$$\rho_{\nu_0}(m, 0) \le \sqrt{2}\,\pi\mathrm{e}\exp\left(-\frac{1}{4}\varepsilon k_m a_1 \phi_0 \sin \phi_0\right), \tag{A.16}$$

where $\phi_0 = \pi/2 - \nu_0$.